Article:
Tin, E., Rutella, S., Khatri, I. et al. (2025) SOCS1 protects acute myeloid leukemia against allogeneic T cell–mediated cytotoxicity. Blood Cancer Discovery, 6 (3). pp. 217-232. ISSN: 2643-3230

https://doi.org/10.1158/2643-3230.bcd-24-0140

SOCS1 protects acute myeloid leukemia against allogeneic T cell-mediated cytotoxicity

Authors: Enoch Tin,[1,2] Sergio Rutella,[3] Ismat Khatri,[1] Yoosu Na,[1] Yongran Yan,[4] Neil MacLean,[4] Jayakumar Vadakekolathu,[3] Mark D. Minden,[4] Aaron D. Schimmer,[4*] JongBok Lee,[1,5*] and Li Zhang[1,2,6*]

Affiliations:

[1]Toronto General Hospital Research Institute, University Health Network; Toronto, Ontario, Canada.

[2]Department of Immunology, University of Toronto; Toronto, Ontario, Canada.

[3]John van Geest Cancer Research Center, School of Science and Technology, Nottingham Trent University; Nottingham, United Kingdom.

[4]Princess Margaret Cancer Centre, University Health Network; Toronto, Ontario, Canada.

[5]Department of Biochemistry and Molecular Biology, University of Calgary; Calgary, Alberta, Canada.

[6]Department of Laboratory Medicine and Pathobiology, University of Toronto; Toronto, Ontario, Canada.

Running title: SOCS1 pathway in AML determines the level of T-cell killing

Additional Information:

***Corresponding authors**

Dr. Li Zhang
Toronto General Hospital Research Institute, University Health Network
101 College St., room 2-207, Toronto, Ontario, M5G 1L7
T. (416) 581-7521 / F. (416) 581-7515
Email: li.zhang@uhnresearch.ca

Dr. Jong Bok Lee
Department of Biochemistry and Molecular Biology, University of Calgary
3330 Hospital Dr. NW, HMRB309, Calgary, Alberta, T2N 4N1
T. (403) 220-8693
Email: jongbok.lee@ucalgary.ca

Dr. Aaron D. Schimmer
Princess Margaret Cancer Centre, University Health Network
101 College St., room 8-706, Toronto, Ontario, M5G 1L7
T. (416) 946-2838
Email: aaron.schimmer@uhn.ca

Conflict of interest disclosures

MDM is a consultant for Astellas, Abbvie, and Celgene. LZ has financial interests (e.g., holdings/shares) in *WYZE Biotech Co Ltd* and previously received research funding and consulting fee/honorarium from the company. ADS has received research funding from Takeda Pharmaceuticals and BMS, and consulting fees/honorarium from Takeda, Astra Zeneca, BMS and Novartis. ADS is a member of the Medical and Scientific Advisory Board of the Leukemia and Lymphoma Society of Canada. SR has received research funding from Wugen, USA and MacroGenics, USA and is an inventor of CD3xCD123 bispecific-related patents for the treatment of hematological malignancies. LZ, JBL, ADS are inventors of DNT cell technology-related patents and intellectual properties for the treatment of AML. The remaining authors have declared no conflicts of interest.

Abstract:

Despite the curative potential of allogeneic hematopoietic stem cell transplantation for acute myeloid leukemia (AML), its efficacy is limited by intrinsic resistance of cancer cells to donor-derived T-cell cytotoxicity. Using a genome-wide CRISPR screening, we identified the SOCS1-JAK1-STAT1 pathway as a mediator of AML susceptibility to T cells. SOCS1 knockdown in AML cells sensitized them to killing by allogeneic double-negative T cells and conventional T cells, whereas SOCS1 overexpression in AML cells induced resistance to T-cell anti-leukemic activity. Mechanistically, SOCS1 protected AML cells from T-cell killing by antagonizing IFNγ-JAK1-induced ICAM-1 expression. Furthermore, AML patients with lower *SOCS1* expression experienced better overall survival, especially those with a lower exhausted $CD8^+$ T-cell score. Thus, this study reveals SOCS1 and its downstream mediators as a potential targetable pathway to enhance T cell-based immunotherapy for AML.

Significance:

Our investigation of the SOCS1 pathway in AML and T-cell interactions provides insights into the clinical inefficacy of JAK inhibitors for AML, suggests SOCS1 as a promising clinical prognostic marker for adoptive T-cell therapy, and demonstrates the potential of targeting SOCS1 and its downstream mediators to enhance the efficacy of T cell-based immunotherapies.

INTRODUCTION

Despite the emergence of molecularly targeted therapies (1), allogeneic hematopoietic stem cell transplantation (allo-HSCT) remains an effective treatment option for patients with high-risk acute myeloid leukemia (AML), and its therapeutic benefit highlights the importance of T cell-mediated immunity in leukemia clearance (2,3). Recently, immune-cell based therapies, particularly chimeric antigen receptor (CAR)-T cell therapy, have achieved significant clinical success in treating B-cell malignancies and multiple myeloma (4). However, as seen in patients treated with allo-HSCT, relapses occur in a significant proportion of patients after CAR-T therapy (5,6). The intrinsic-resistance mechanisms by which leukemic cells evade T-cell immunity, leading to disease relapse, are not completely understood (7,8). Investigating the interactions between leukemic cells and T cells has the potential to reveal underlying cancer-resistance mechanisms and provide strategies to reduce disease relapse.

$CD3^+CD4^-CD8^-$ double-negative T cells (DNTs) constitute 1%-5% of peripheral lymphocytes in humans (9,10). Previously, we demonstrated that *ex vivo* expanded DNTs from healthy donors are effective at targeting allogeneic AML cells without alloreactivity against healthy tissue, primarily through MHC-independent mechanisms involving NKG2D and DNAM-1 (9,10). Furthermore, the feasibility, safety, and potential efficacy of allogeneic DNTs were demonstrated in a phase I clinical trial with high-risk AML patients who relapsed after allo-HSCT (11). However, four out of ten patients in the phase I trial failed after DNT therapy regardless of dosing (11). Additionally, we have found that ~30% of primary AML samples resist DNT-mediated cytotoxicity through unclear mechanisms (9). A better understanding of cytotoxic pathways during AML and DNT interactions may help identify targetable molecules

and clinical biomarkers to improve DNT therapy and potentially other T cell-based treatments for AML.

Suppressors of cytokine signaling (SOCS) family proteins consist of eight members that are key negative regulators of Janus kinase–signal transducer and activator of transcription (JAK-STAT) pathways (12,13). Cytokines typically activate specific JAK proteins, which phosphorylate corresponding STAT molecules, resulting in phosphorylated STAT (pSTAT) nuclear translocation and changes in transcriptional activity within the cell (12,13). These signals can be antagonized by an individual or combination of SOCS members through distinct mechanisms (12,13). SOCS1 is a direct inhibitor of multiple JAK family proteins and involved in numerous interferon and interleukin signaling pathways (12–14). Although SOCS1 is generally recognized as a tumor suppressor and is frequently repressed in AML and other cancers through hypermethylation (15,16), high levels of SOCS1 have been associated with high-risk AML mutations and tumor protection against cytokine-mediated growth inhibition (17,18). Likewise, abnormally increased JAK-STAT signaling has been well characterized in human leukemias (12,19), yet JAK inhibitors have demonstrated limited efficacy in treating AML patients (20–22). Whether these observations relate to the influence of SOCS1 in AML susceptibility to T-cell immunity is currently unknown.

In this study, we uncovered a mechanism that mediates the resistance of AML cells to T-cell killing, using DNTs as a surrogate and T_{conv} cells for validation. We discovered that during the interactions between AML and T cells, SOCS1 expression in AML increases leukemia blast resistance to T cell-mediated cytotoxicity by limiting JAK1 activation and subsequent intercellular adhesion molecule-1 (ICAM-1) upregulation. This data provides a mechanism to

explain the clinically and immunologically significant role of SOCS1 in AML and demonstrate the potential of adoptive T-cell therapy with SOCS1 inhibitors.

RESULTS

Intrinsic SOCS1 expression level in AML regulates its susceptibility to T-cell killing

To systematically explore genes and pathways crucial for AML-intrinsic resistance to T cell-mediated killing, we performed a genome-wide CRISPR screen using $Cas9^+$ OCI-AML2 cell line cultured with or without DNTs (Supplementary Fig. S1A and Supplementary Fig. S1B). The remaining live OCI-AML2 cell line after the co-culture were isolated and sent for next-generation sequencing to identify sgRNAs that were enriched or depleted in AML cells co-cultured with DNTs, relative to the untargeted AML control group. By comparing the number of sgRNA to those in AML cells cultured alone, sgRNAs targeting the essential genes for AML survival without the influence of DNTs were excluded. Consistently across triplicates, the targets of sgRNAs that were enriched in DNT-targeted AML cells represented genes that conferred susceptibility to T-cell killing and vice-versa (Fig. 1A and Supplementary Figs. S1C-S1E). From the screen, a SOCS1-specific pathway was identified in AML (Fig. 1A and Supplementary Table S1) which involved SOCS1 and its potential target pathway, IFNGR-JAK1-STAT1 (Fig. 1B) (12–14). Notably, knockout (KO) of SOCS1, IFNGR, JAK1, or STAT1 did not affect AML cell viability based on the transduced, untargeted AML group (Supplementary Fig. S1F).

There is limited understanding of the role of SOCS1 expression in AML cells regarding patient survival, especially in the context of AML and T-cell interactions. Thus, we first tested whether genetically inhibiting SOCS1 in AML cells could render them more susceptible to T cell-mediated cytotoxicity by knocking down SOCS1 in KG-1a cells (Supplementary Fig. S2), an AML cell line known to be highly resistant to T-cell killing (23,24). Compared to scramble controls, SOCS1 knockdown ($SOCS1^{KD}$) KG-1a cells were effectively killed by DNTs (Fig. 1C, top). Similar results were seen with mixed $CD4^+$ and $CD8^+$ T_{conv} cells (Fig. 1C, bottom),

suggesting the expression of SOCS1 in AML is important for T cell-mediated cytotoxicity *in vitro*. Importantly, $SOCS1^{KD}$ in primary AML blasts (Supplementary Fig. S3; n=3) increased their susceptibility to DNT-mediated cytotoxicity (Fig. 1D). To examine the role of SOCS1 in regulating AML susceptibility to T cells *in vivo*, mice were engrafted with control or $SOCS1^{KD}$ KG-1a cells followed by treatment with DNTs or vehicle control (Fig. 1E). DNTs were unable to reduce the engraftment of control KG-1a cells, as previously observed (23,24), but significantly decreased the engraftment of $SOCS1^{KD}$ KG-1a cells (Fig. 1F). This demonstrates that inhibiting SOCS1 expression in AML cells increases their susceptibility to T-cell immunity, including otherwise T cell-resistant AML cells.

To further explore the importance of SOCS1 expression in AML, we tested whether SOCS1 overexpression ($SOCS1^{OE}$) in DNT-susceptible AML cell lines (24) would render them resistant to T cells. Overexpression of SOCS1 in OCI-AML2 and MV4-11 (Supplementary Fig. S4) significantly increased their resistance to DNT and T_{conv} cell anti-leukemic effects in an overnight killing assay (Fig. 1G). $SOCS1^{OE}$ OCI-AML2 cells, which express CD4 (Supplementary Fig. S5A), also exhibited resistance to anti-CD4 CAR (CAR4)-DNTs and CAR4-$CD8^+$ T cells (Supplementary Figs. S5B-D). Of note, we did not observe changes in the level of T-cell cytotoxicity against control compared to $SOCS1^{OE}$ OCI-AML2 cells in a short 2-hour assay (Supplementary Fig. S6), suggesting that SOCS1-mediated effects occur through a slower kinetic mechanism. Consistent with this finding, DNTs failed to reduce AML engraftment in mice infused with $SOCS1^{OE}$ MV4-11 cells, while effectively reducing the AML engraftment level in the control group (Fig. 1H and Fig. 1I). Notably, overexpressing or knocking down SOCS1 did not alter the sensitivity of AML cell lines and primary AML samples to daunorubicin or venetoclax (Supplementary Fig. S7A and Supplementary Fig. S7B), common therapeutic

approaches for AML (1,2), suggesting that SOCS1 specifically influences the sensitivity of AML cells to immune cell-mediated anti-leukemic activity.

To assess whether SOCS1 levels can predict the susceptibility of AML cells to T cells, we studied the correlation between SOCS1 gene expression in AML cell lines and primary AML blasts and their susceptibility to DNT-mediated cytotoxicity. *SOCS1* expression level negatively correlated with the susceptibility of AML cells to DNT-mediated cytotoxicity (Fig. 1J). However, the expression of other SOCS family members, such as *SOCS3* and *CISH* (13), did not show any correlation (Supplementary Fig. S8A), nor were they significant hits from the CRISPR screen (Supplementary Fig. S8B). Collectively, these data demonstrate that SOCS1 expression level determines and predicts the susceptibility of AML cells to T cells *in vitro* and *in vivo*.

JAK1 activity, but not expression level, correlates with AML resistance to T-cell killing

From the CRISPR screen, the JAK1-STAT1 axis was the top target candidate to explain previous SOCS1 effects (Fig. 1A) (14). To examine the impact of JAK1 inhibition, AML cell lines were transduced with shRNAs against JAK1 (Supplementary Fig. S9A) or treated with a JAK1 inhibitor, itacitinib, followed by co-incubation with T cells. Although no changes in growth kinetics and viability were observed in almost all cases between control and JAK1-inhibited AML *in vitro* (Supplementary Fig. S9B and Supplementary Fig. S9C), reduced levels of T cell-mediated killing were observed against JAK1-silenced AML cell lines, OCI-AML2 and MV4-11 (Fig. 2A), and itacitinib-treated AML cell lines (Fig. 2B) and primary AML blasts (n=5; Fig. 2C). Furthermore, knocking down JAK1 in MV4-11 cells rendered them resistant to the anti-leukemic activity of DNTs in an *in vivo* AML xenograft model (Fig. 2D and Supplementary Fig. S10). $JAK1^{KD}$ MV4-11 cells harvested from mouse femurs continued to be more resistant to T cells than their control counterparts in an *ex vivo* cytotoxicity assay (Fig. 2E).

Despite our results indicating that JAK1 promotes the susceptibility of AML cells to T cells, the JAK1 expression level in AML cells was inversely correlated with their susceptibility to DNTs (Supplementary Fig. S11A). The AML cell line that is most resistant to DNTs, KG-1a (23,24), expressed the highest level of JAK1 (Supplementary Fig. S11A). Additionally, *JAK1* expression level did not correlate with AML patient survival (Supplementary Fig. S11B). To determine if JAK1 activity, rather than its expression level, predicts the susceptibility of AML cells to T cells, we measured the phosphorylation level of STAT1, the major downstream molecule of JAK1 (12,13). We found that the fold increase in pSTAT1 level in AML cells after co-culture with DNTs correlated with their susceptibility to DNT-mediated cytotoxicity (Fig. 2F and Supplementary Figure S12). Overall, these results support the contention that the activity of JAK1-STAT1 signaling, rather than JAK1 expression levels per se, is important in regulating the susceptibility of AML cells to T cell-mediated killing.

T-cell effector function against AML is dependent on the SOCS1-JAK1 axis

To examine whether SOCS1 effects depend on JAK1-STAT1 activity in AML and T-cell interactions, DNTs were co-cultured with $SOCS1^{OE}$, $SOCS1^{KD}$, or control AML cells followed by pSTAT1 staining (Supplementary Fig. S12). The expression of pSTAT1 in $SOCS1^{OE}$ AML cells was significantly lower than that of the control in the presence of DNTs (Fig. 3A). In line with this, the level of pSTAT1 was significantly higher in $SOCS1^{KD}$ KG-1a cells in the presence of DNTs relative to the control (Fig. 3B).

Given that IFNγ is a known activator of the JAK1-STAT1 pathway (25), we treated AML cells with recombinant IFNγ (rIFNγ) or vehicle control and assessed pSTAT1 levels and AML susceptibility to DNTs. As previously reported, rIFNγ increased pSTAT1 levels (Supplementary Fig. S13) (25) and sensitizes AML cells to DNT-mediated cytotoxicity (9). We also

demonstrated that IFNγ-mediated sensitization of AML cells to DNTs is JAK1-dependent, as knocking down JAK1 abrogated the effect of IFNγ on DNT-mediated cytotoxicity against AML cells (Supplementary Fig. S14).

To determine whether SOCS1 increases AML resistance to T cells by acting on the JAK1-STAT1 pathway, $SOCS1^{OE}$ AML cells were stimulated with rIFNγ. In $SOCS1^{OE}$ AML cells, rIFNγ was less effective at inducing pSTAT1 expression, confirming that SOCS1 inhibits the JAK1-STAT1 pathway in AML cells (Fig. 3C). Consistent with this, overexpression of SOCS1 reduced the sensitization of AML cells to T cells through the JAK1 pathway activated by rIFNγ (Fig. 3D), while SOCS1 knockdown enhanced these effects (Fig. 3E) compared to their respective controls. Of note, treatment with rIFNγ induced minimal changes in AML viability relative to control cells regardless of their SOCS1 expression levels (Supplementary Fig. S15), suggesting that rIFNγ is priming AML cells to T-cell mediated cytotoxicity rather than directly inducing AML cell death. We also found a significant inverse correlation between the degree of rIFNγ-mediated sensitization to DNTs and *SOCS1* expression in AML cell lines and primary AML blasts (Fig. 3F). It is important to note that no significant changes were detected in IFNγ concentration in the supernatants of DNTs co-cultured with $SOCS1^{OE}$ and $JAK1^{KD}$ AML cells relative to their respective controls (Supplementary Fig. S16), suggesting that SOCS1 and JAK1 expression do not affect IFNγ production. Notably, similar to IFNγ, TNFα and IFNα, which also activate JAK1 (25,26), do not induce AML cell death (Supplementary Fig. S17A) but sensitize AML cells to DNT killing in a SOCS1-dependent manner (Supplementary Fig. S17B-D). Altogether, these findings demonstrate that the specific interplay between SOCS1 and JAK1 activation in AML cells modifies the sensitivity of AML to T-cell killing.

ICAM-1 is crucial for the SOCS1-JAK1 axis to alter AML sensitivity to T-cell killing

To elucidate the cytotoxic mechanisms regulated by the SOCS1-JAK1 pathway, SOCS1^{OE} AML cells were compared with controls stimulated with rIFNγ to activate JAK1 and stained for cytotoxic molecules known to be involved in DNT and T_{conv}-cell anti-leukemic functions (9,24,27,28). Among these molecules, ICAM-1 expression was most drastically increased on AML cells and subsequently reduced by SOCS1 overexpression (Fig. 4A and Supplementary Fig. S18). Notably, ICAM-1 was one of the top susceptibility genes from the CRISPR screen, as shown in Figure 1A.

A recent study demonstrated the importance of ICAM-1 in determining the susceptibility of AML cells to T-cell killing, but the mechanisms involved in the regulation of ICAM-1 were unclear (28). To explore the connection between SOCS1 and ICAM-1 expression, ICAM-1 levels were measured on SOCS1^{OE} OCI-AML2 and MV4-11 and SOCS1^{KD} KG-1a cells after co-culture with T_{conv} cells and DNTs. The magnitude of ICAM-1 upregulation induced by T cells (Fig. 4B) and CAR4-T cells (Supplementary Fig. S19) was significantly lower in SOCS1^{OE} AML cells and significantly greater in SOCS1^{KD} KG-1a cells (Fig. 4C) relative to respective controls. A similar reduction in T cell-mediated ICAM-1 expression was observed in JAK1-silenced AML cells (Supplementary Fig. S20). Furthermore, we detected significantly higher expression of ICAM-1 on control MV4-11 cells compared to SOCS1^{OE} MV4-11 cells in the bone marrow (BM) of MV4-11-engrafted mice treated with DNTs (Fig. 4D), which may explain why DNTs can effectively lower AML engraftment in the control group compared to the SOCS1^{OE} group. In addition, a significant inverse correlation between IFNγ-induced ICAM-1 upregulation and *SOCS1* expression in AML cell lines and primary AML blasts were observed (Fig. 4E). Thus, these results demonstrate that SOCS1 inhibits ICAM-1 upregulation induced by JAK1 signaling.

To investigate the functional significance of SOCS1 regulation on ICAM-1 expression in AML and T-cell interactions, $SOCS1^{KD}$ and control KG-1a cells were co-incubated with DNTs in the presence of neutralizing antibodies against ICAM-1 or an isotype control. The sensitizing effects of SOCS1 silencing were abrogated by anti-ICAM-1 antibodies (Fig. 4F). Moreover, we tested the impact of JAK1-signaling activation via rIFNγ in ICAM-1^{KO} OCI-AML2 cells and its control (Supplementary Fig. S21). ICAM-1^{KO} abrogated the effect of JAK1 signaling on the sensitization of OCI-AML2 cells to DNTs (Fig. 4G). Consistent with this, neutralizing antibodies against ICAM-1 effectively reduced the rIFNγ-induced JAK1 sensitizing effects in AML cell lines (Fig. 4H) and 4 out of 5 primary AML blasts (Fig. 4I) to T cell-mediated cytotoxicity. The antibody showed minimal effects on the viability of AML in the absence of T cells (Supplementary Fig. S22). Additionally, the degree of ICAM-1 upregulation significantly correlated with an increased level of AML sensitivity caused by JAK1 pathway activation (Fig. 4J). Similarly, the sensitization effects of AML by $SOCS1^{KD}$ and JAK1 activation via rIFNγ were effectively abrogated by using a neutralizing antibody against lymphocyte function-associated antigen-1 (LFA-1; Supplementary Fig. S23A and Supplementary Fig. S23B), a high affinity ICAM-1 receptor highly expressed on DNTs and other effector cells (27,29–32). Taken together, these findings demonstrate the relationship between the activity of the SOCS1-JAK1 axis and ICAM-1 expression on AML cells to alter T-cell effector function against AML.

SOCS1 inversely correlates with AML patient survival without affecting disease burden

To establish the clinical relevance of SOCS1, we examined large patient cohorts with *de novo* AML. In The Cancer Genome Atlas (TCGA) AML cohort (n=161 cases), we found that patients with lower than median *SOCS1* expression exhibited significantly better survival compared to those with higher than median *SOCS1* levels (Fig. 5A). This was also observed in

select TCGA solid tumor types, such as kidney renal clear cell carcinoma and lower grade glioma (Supplementary Fig. S24A). An additional AML cohort, the Princess Margaret Cancer Center (PMCC) cohort (n=287 cases), independently validated the prognostic relevance of SOCS1 (Fig. 5B) regardless of whether patients were censored at the time of allo-HSCT (Supplementary Fig. S24B), which indicates that survival trends were not due to differences in treatment intensity. As seen with *JAK1*, *ICAM-1* and *IFNG* levels could not be linked to patient survival (Supplementary Fig. S25A and Supplementary Fig. S25B), and *ICAM-1* levels remained similar in $SOCS1^{high}$ and $SOCS1^{low}$ patient groups (Supplementary Fig. S25C). This continues to indicate that the activity of the JAK1-STAT1 signaling pathway regulated by SOCS1 is of greater importance for immune-susceptibility in AML and patient survival rather than the basal expression of *ICAM-1* or *IFNG*. This may be partly contributed by the transient expression of inducible ICAM-1 (Supplementary Fig. S25D) and the pleiotropic effect of IFNγ harboring both anti- and pro-tumorigenic effects (33–35).

Consistent with our observation that SOCS1 expression does not affect AML cell proliferation *in vitro* (Supplementary Fig. S26), disease burden was not significantly different between $SOCS1^{high}$ and $SOCS1^{low}$ patient groups in the PMCC cohort (Fig. 5C). The lack of SOCS1 activity on AML proliferation was further supported by similar *in vivo* BM engraftment levels of $SOCS1^{OE}$ and $SOCS1^{KD}$ AML cells compared with their respective controls (Fig. 5D). Furthermore, patients achieving complete remission or experiencing primary induction failure after standard-of-care chemotherapy have similar SOCS1 levels at baseline (Supplementary Fig. S27), providing more evidence that the survival benefit of SOCS1 is not due to affecting AML responsiveness to chemotherapy as observed in Supplementary Figure S7. Supportive of our findings that SOCS1 affects AML susceptibility to T cell-mediated killing, bulk RNA-

sequencing revealed significant depletion of general immune response pathways in SOCS1^{OE} AML (Fig. 5E, Supplementary Table S2, and Supplementary Table S3). This suggests that SOCS1 activity in AML cells is important for sustaining anti-AML immunity in patients.

Re-analysis of a legacy single-cell RNA-sequencing dataset encompassing 214,417 BM cells from 42 patients with newly diagnosed AML (36), indicated the occurrence of a higher number and an increased strength of inferred cellular interactions in SOCS1^{low} cells relative to SOCS1^{high} cells (Fig. 5F). Specifically, higher overall interactions were predicted between hematopoietic stem cells (HSCs) and CD8$^+$ and CD4$^+$ T_{conv} cells in SOCS1^{low} BM cells (Fig. 5G), in which annotated "HSCs" showed high expression of genes associated with quiescent leukemic stem cells, consistent with their malignant status (Supplementary Fig. S28). Further *in silico* modeling of cellular crosstalk in SOCS1^{low} BM cells also suggested higher CD4$^+$ effector memory and lower CD4$^+$ regulatory T-cell interactions through HLA class II molecules on HSCs (Supplementary Fig. S29), all of which may influence CD8$^+$ T-cell effector function.

Given the increased level of T-cell interactions among SOCS1^{low} BM cells, we further assessed the impact of T-cell activity in the context of SOCS1 expression within the PMCC cohort. SOCS1^{low} patients (Supplementary Fig. S30) with a lower exhausted CD8$^+$ T-cell score (34), indicating the presence of functional T cells, experienced improved survival (Fig. 5H, left). However, this was not observed in SOCS1^{high} patients (Fig. 5H, right), suggesting an influence of SOCS1 expression on T-cell efficacy. Overall, these data support that T cell-mediated immunity contributes to the prolonged survival observed in AML patients with lower SOCS1 expression.

DISCUSSION

In this study, we discovered that SOCS1 in AML cells regulates their susceptibility to T-cell killing by dampening JAK1 signaling and reducing inducible ICAM-1 levels (Fig. 5I). Clinically, low SOCS1 correlates with a better AML patient survival without directly affecting disease burden, particularly in patients whose BM-infiltrating $CD8^+$ T cells exhibited a lower exhaustion score. These results highlight the significance of the SOCS1 pathway in regulating T-cell mediated anti-leukemic activity and the beneficial role of T cells in the improved survival observed among $SOCS1^{low}$ AML patients.

Cancer immune-resistance continues to be one of the main challenges that hinder the success of cancer immunotherapy (7). Several studies have turned to *in vitro* and *in vivo* CRISPR screens to systematically pinpoint genes required for T cells to effectively engage cancer cells (37–39). Two *in vivo* mouse CRISPR screens briefly highlighted SOCS1 as one of the resistance genes that protect solid tumors and B-cell leukemias from the anti-tumoral activities of T cells (38) and CAR-T cells (39), respectively. However, clinical and functional investigations were not performed to determine the involvement of SOCS1 in cancer cell and T-cell interactions in these studies (38,39). Filling this knowledge gap, our study functionally demonstrates the importance of SOCS1 in AML cells to shape their susceptibility to T_{conv} cells and DNTs and reveals the role of the JAK1-STAT1-ICAM-1 pathway, regulated by SOCS1, in AML and T-cell interactions. Here, we showed that silencing SOCS1 in a highly T-cell resistant AML cell line could render these AML cells more susceptible to T-cell anti-leukemic effects *in vitro* and *in vivo*. These findings warrant further exploration of SOCS1 mechanisms in the interactions between CAR-T cells and a variety of solid or liquid tumor targets to overcome tumor immune resistance.

The pro- and anti-tumorigenic role of SOCS1 in AML remains controversial. Similar to other leukemias, SOCS1 has been portrayed as a tumor suppressor as SOCS1 gene methylation and other SOCS1 repression mechanisms cause increased JAK-STAT signaling, contributing to AML development (16,40). While this suggests that reduced SOCS1 expression supports the development of AML, we found that there was better survival among AML patients with lower *SOCS1* levels in two independent cohorts. These results are consistent with superior survival of $SOCS1^{low}$ AML patients in another *de novo* AML cohort as reported by Hou *et al.* (17). However, the mechanisms by which SOCS1 impacts patient survival were not fully understood, with some studies reporting associations with high-risk AML mutations and protective effects against cytokine-mediated growth inhibition (17,18). Here, we establish that SOCS1 significantly alters AML susceptibility to T-cell immunity. Interestingly, $SOCS1^{low}$ patients in the PMCC cohort were predominantly comprised of patients with intermediate- and adverse-risk characteristics (Supplementary Fig. S30), who have been described to experience no survival benefits or to even experience a worse prognosis with increased T-cell infiltration, respectively (34). However, we observed a significant survival benefit in $SOCS1^{low}$ patients with a lower exhausted $CD8^+$ T-cell signature, suggesting that SOCS1 may play an important role in the presence of more functional T cells, despite the presence of clinically unfavorable cytogenetic features. In keeping with our data, higher percentages of patient-derived T cells dividing after *in vitro* anti-CD3 stimulation at the time of diagnosis have been linked to longer survival in patients with AML (41), reinforcing the concept that T-cell function contributes to the disease outcome in response to standard-of-care induction chemotherapy (42). Our results further explored *in silico* modeling of cellular interactions from single-cell RNA-sequencing data, which predicted elevated $CD8^+$ and $CD4^+$ signaling in specimens with a $SOCS1^{low}$ tumor microenvironment.

Effective T-cell responses require functional immune synapse formation and are important for AML patient survival (43). Unfortunately, $CD8^+$ T cells from AML patients form defective immune synapses, leading to the inability to properly engage AML cells (43). Several studies have demonstrated that the interaction between ICAM-1 and its receptor, LFA-1, is crucial for T cells, including CAR-T_{conv} cells and CAR-DNTs, to form immune synapses with malignant cells and kill them (28,44–46). Consistent with this, Sayitoglu *et al.* recently reported that AML cells expressing high levels of ICAM-1 were sensitive to engineered $CD4^+$ and primary $CD8^+$ T cell-mediated cytotoxicity (28). Blocking ICAM-1 on AML cells was sufficient to reduce T-cell killing of AML cells (28), consistent with our findings in DNTs. However, the molecular mechanisms regulating ICAM-1 expression in AML were not described. Here, we demonstrated that SOCS1 inhibits JAK1 signaling to prevent ICAM-1 upregulation, and the degree of ICAM-1 upregulation negatively correlates with SOCS1 expression while positively correlating with T cell-mediated cytotoxicity. As a result, examining SOCS1 levels in AML patients may predict the efficacy of T-cell based immunotherapies.

In hematological malignancies, JAK mutations and abnormal activation have been generally recognized as key disrupting factors in normal hematopoietic processes (19). JAK inhibitors demonstrate potent anti-leukemic activity in mouse AML models (47). Despite promising preclinical results, several clinical trials using JAK1/2 inhibitors showed limited efficacy in patients with AML and other hematological cancers, leading to the termination of some trials (20–22). Our data demonstrate that inhibiting JAK1 in AML cells can significantly increase their resistance to T cell-mediated killing by limiting ICAM-1 upregulation. While JAK1 inhibitors may reduce AML engraftment *in vivo*, JAK1 inhibition may counteract any

388 immune-mediated anti-tumoral effects, thereby contributing to the lack of observed clinical
389 efficacy of JAK1/2 inhibitors in AML patients.

390 Our data suggest that activating the JAK1 pathway or inhibiting SOCS1 activity in cancer
391 cells synergize with T-cell based immunotherapies like adoptive T-cell therapy. For instance,
392 interferons and Stimulator of Interferon Genes (STING) agonists have been shown to activate
393 JAK1 and demonstrated direct and indirect anti-tumor activity against AML (25,48) with the
394 potential of reversing the immune-resistant phenotype of AML blasts from patients who relapsed
395 after allo-HSCT (35). STING agonists are currently being evaluated in clinical trials for various
396 cancers with promising results when combined with PD-1 checkpoint inhibitors (49), while
397 commercially available SOCS1 antagonists have not been developed or clinically tested. Thus,
398 combining SOCS1 antagonists or JAK1 activators, such as STING agonist, with adoptive T-cell
399 therapies might be an effective strategy to yield potent anti-cancer effects in AML patients.

400 Despite the survival benefit mediated by T-cell immunity in AML patients receiving allo-
401 HSCT, the regulation of interactions between T cells and AML cells remains largely unknown.
402 Our study identified a SOCS1 pathway as a clinically relevant mediator that dictates how T cells
403 engage with AML cells through ICAM-1. The study also provides insights into why AML
404 patients with lower SOCS1 levels have improved survival and supports the components of the
405 SOCS1 pathway as potential biomarkers to identify patients more likely to respond to T-cell
406 based therapies or as targets to increase the efficacy of adoptive DNT and T_{conv}-cell therapy.
407

MATERIALS AND METHODS

Expansion of DNTs and T_{conv} cells

Ex vivo expansion of DNTs was previously described (9,10). Briefly, DNTs were isolated from peripheral blood mononuclear cells (PBMCs) of healthy donors through Ficoll (Lymphoprep; STEMCELL Technologies) centrifugation followed by $CD4^+$ and $CD8^+$ depletion (RosetteSep; STEMCELL Technologies). On day 0-3, DNTs were cultured on anti-CD3 antibody-coated plates (5 mg/mL, OKT3; Miltenyi Biotec; RRID: AB_1036144), followed by soluble anti-CD3 (0.1 μg/mL) on days 7-20, in RPMI-1640 (ThermoFisher) supplemented with 10% fetal bovine serum (FBS, ThermoFisher) or AIM-V (ThermoFisher) and 250 IU/mL of IL-2 (PROLEUKIN, Novartis Pharmaceuticals). Phenotypic purity of DNTs was examined on days 10 and 14, and DNTs from day 10-20 of cultures were used in the experiments. For T_{conv}-cell expansion, PBMCs cultured in RPMI-1640 with 10% FBS were stimulated with ImmunoCult™ Human CD3/CD28 T cell activator (STEMCELL Technologies), in accordance with manufacturer protocols. CAR4-T cells were generated as previously described (46), transducing *ex vivo* DNTs and $CD8^+$ T cells on day 3 of expansion using a 2^{nd} generation retroviral CAR construct. Empty retroviral vectors were used as controls.

Cell lines and primary samples

AML cell lines OCI-AML3 (RRID: CVCL_1844), OCI-AML2 (RRID: CVCL_1619), KG-1a (RRID: CVCL_1824), MV4-11 (RRID: CVCL_0064), and U937 (RRID: CVCL_0007) were obtained from American Type Culture Collection. OCI-AML2 and MV4-11 were cultured in IMDM (ThermoFisher), OCI-AML3 in alpha-MEM (ThermoFisher), and KG-1a and U937 in RPMI-1640 (ThermoFisher). All cultures were supplemented with 10% FBS. Regular *Mycoplasma* testing was last performed by qPCR (Charles River Research) in 2023, and cell

lines were used within 1 month of thawing from frozen vials for experiments. Primary AML samples cryopreserved in 50% DMSO, 10% FBS, and alpha-MEM were obtained from the Princess Margaret Leukemia Bank and frozen in liquid nitrogen until use. Only samples with >30% viability prior to the start of the experiment were used. Patient sample information is provided in Supplementary Table S4. Race and ethnicity of samples were not available. All cells were incubated at 37°C, 5% CO_2.

Antibodies and flow cytometry

The following anti-human antibodies and dyes (BioLegend) were used: CD3 (HIT3a; RRID: AB_314052), CD56 (HCD56; RRID: AB_604101), CD4 (RPA-T4; RRID: AB_2562052), CD8 (HIT8a; RRID: AB_314115), CD33 (WM53; RRID: AB_314351/AB_2734264), CD34 (581; RRID: AB_1731862), CD45 (HI30; RRID: AB_314402), CD54 (HA58; RRID: AB_10900254/AB_10917389), phospho-STAT1 (Tyr107, A17012A; RRID: AB_2734525), Annexin-V (RRID: AB_1279044), DAPI (Cat#: 422801), and Zombie Violet fixable dye (Cat#: 423113). Data acquisition was performed using the Attune NxT Flow Cytometer (ThermoFisher), followed by analysis with FlowJo software (Tree Star; RRID: SCR_008520).

Flow cytometry-based in vitro cytotoxicity assays

Ex vivo expanded DNTs and T_{conv} cells were co-cultured with AML cell lines (for 2, 24 hours, or multiple days) or primary AML cells (for 3 or 24 hours) to measure the cytotoxic activities of T cells. The effector-to-target (E:T) ratios are indicated in the figure legends. AML viability was determined by Annexin-V (for 2- to 24-hour assays) or DAPI (for multi-day assays) in $CD3^-CD33^+$ or $CD3^-CD34^+$ gated populations for AML cell lines and $CD45^{low}CD3^-CD33^+$ or

CD34^{+} populations for primary AML samples (Supplementary Fig. S31 and Supplementary Fig. S32). Percentage specific killing was calculated by $\frac{\%\ Dead_{with\ T\ cells} - \%\ Dead_{without\ T\ cells}}{100 - \%\ Dead_{without\ T\ cells}}$ x 100%.

For pre-treatment assays, AML cells were treated with recombinant human IFNγ (50 ηg/mL or specified; BioLegend) or itacitinib (10μM; Selleckchem) for 24 hours and washed with phosphate-buffered saline (PBS) prior to the killing assay. To assess the effect of JAK1 inhibition, AML cells and DNTs were co-cultured with added itacitinib. For ICAM-1 or LFA-1 blocking assays, anti-CD54 (5 μg/mL, HCD54; BioLegend; RRID: AB_535974), anti-CD18 (5 μg/mL, TS1/18; BioLegend; RRID: AB_2561483), or IgG1 isotype control (BioLegend) were added to the cytotoxicity assay. The absolute percentage increase in killing was calculated by $\%\ Specific\ Killing_{treated} - \%\ Specific\ Killing_{untreated}$ to determine treatment effects on T-cell killing of AML.

Phosphorylated STAT1 intracellular staining

AML targets were co-incubated with DNTs (for 2 or 24 hours) or treated with rIFNγ (for 10 mins or 24 hours). After, cells were stained with Zombie Violet fixable dye (BioLegend) and surface anti-human antibodies previously listed. Subsequently, cells were fixed and permeabilized with fixation buffer (BioLegend) and True-Phos^{TM} perm wash buffer (BioLegend), respectively. The fixed and permeabilized cells were intracellularly stained using anti-human phospho-STAT1 (Tyr107, A17012A; BioLegend).

Enzyme-linked immunosorbent assay (ELISA)

DNTs and AML targets were co-incubated at an E:T ratio of 1:1 for 2 hours. After, the supernatants were collected and used for ELISA with anti-human IFNγ (B27), as previously described (9).

Genome-wide CRISPR Screen

A genome-wide CRISPR/Cas9 KO screen was performed in OCI-AML2 cells stably expressing Cas9 to identify genes that conferred sensitivity and resistance to DNT-mediated killing. OCI-AML2 cells were transduced with a Cas9 in a lentiviral vector, Lenti-Cas9-2A-Blast (RRID: Addgene_73310) (50). A stable population of cells were selected with blasticidin (10 μg/mL) for 6 days. Single-cell clones were obtained by plating in a 96-well plate at a density of 0.4 cell/well, and a clonal population with high Cas9 expression was selected. $Cas9^+$ OCI-AML2 cells were transduced with a pooled library (90k library) of 91,320 gRNAs in lentiviral vectors targeting 17,232 genes at a ratio of 6 gRNAs per gene, similar to previously described (50). These cells were transduced at a multiplicity of infection of approximately 0.3–0.4 to obtain coverage of at least 200-fold per gRNA. One day post-transduction, cells were treated with puromycin (2 μg/mL) for 48 hours to select transduced cells. Cells were then treated with DNTs at their IC_{80} (E:T ratio of 1:1) for 18 days. Genomic DNA was then extracted from cell populations; gRNA sequences were amplified by PCR and sequenced on an Illumina Hiseq2500. Data were analyzed using MAGeCK method (RRID: SCR_025016).

Gene silencing in AML cell lines

To silence JAK1 in AML cell lines, shRNA JAK1 sequence (CGTTCTCTACTACGAAGTGAT) and control vector (CGAGGGCGACTTAACCTTAGG) were cloned into lentiGuide-Puro (RRID: Addgene_52963) vectors, as previously described (24,27). These sequences were kindly provided by Dr. Hansen He's laboratory from University Health Network (UHN). For SOCS1 silencing in AML cell lines, we used the shRNA eGFP SOCS1 vector (NM_003745.1) and scrambled control (GeneCopoeia). Lentiviral particles with the appropriate shRNA were generated in HEK293T cells (Invitrogen; RRID: CVCL_0063) using pMDG.2 (RRID: Addgene_12259) and psPAX2 packaging plasmids (RRID:

Addgene_12260). Wild-type (WT) AML cells were transduced, for 48 hours, followed by puromycin selection for 72 hours at 1 μg/mL for OCI-AML2 and MV4-11. KG-1a cells were sorted by fluorescence-activated cell sorting to purify SOCS1-silenced GFP^+ KG-1a cells.

SOCS1 knockdown in primary AML

Lentiviral particles were generated in HEK293T cells using pMDG.2 (RRID: Addgene_12259), pMDLg/pRRE (RRID: Addgene_12251), and pRsv-Rev packaging plasmids (RRID: Addgene_12253), concentrated using Lenti-X™ Concentrator (Takara), and resuspended in HBSS (Gibco) with 25 mM HEPES (ThermoFisher). To transduce primary AML cells, 6-well plates were coated with RetroNectin® (20 μg/mL in PBS; Takara) and then blocked with 2% bovine serum albumin (BSA; Sigma) in PBS (W/V). The BSA solution was then aspirated, and concentrated lentiviral particles in HBBS with 25 mM HEPES were added to each well. To promote the attachment of lentiviral particles to RetroNectin, the plate was centrifuged at 3,000 RPM for 2 hours at 32°C. Next, viral supernatant was aspirated. Primary AML cells were resuspended at $5x10^5$ cells/mL in X-VIVO 10 (Lonza) with 20% BIT (STEMCELL Technologies) supplemented with growth factors (50 ηg/ml, FLT3-L; 10 ηg/mL, IL6; 50 ηg/mL, SCF; 25 ηg/mL, TPO; 10 ηg/mL, IL3; 10 ηg/mL, G-CSF; PeproTech) and protamine sulfate (5 μg/mL; MP Biomedical). $2x10^6$ cells primary AML cells were added to each virus-coated well to reach a transduction rate of 20-30%. To promote the interaction between the cells and lentiviral particles, the plate was centrifuged again at 2000 RPM for 10 mins at room temperature and then transferred to a 37°C incubator to initiate lentiviral transduction. 24 hours after incubation, cells were resuspended in fresh media at $1x10^6$ primary AML cells/mL and cultured in a new 6-well plate.

SOCS1 overexpression in AML

To overexpress SOCS1 in AML, we used lentiviral vector EX-K2201-Lv105-10 expressing ORF SOCS1 (NM_003745.2) and a control vector (GeneCopoeia) to generate lentiviral particles in HEK293T cells. OCI-AML2 and MV4-11 WT cells were transduced for 48 hours, followed by puromycin selection for 72 hours at 1 μg/mL.

CRISPR knockout of ICAM-1 in OCI-AML2

Stable Cas9-expressing OCI-AML2 cell lines were generated as previously described (24,27). Briefly, Cas9-GFP lentiviral particles were produced in HEK293T cells using pMDG.2 and psPAX2 packaging plasmids. After a 24-48-hour transduction period, $Cas9^{+}GFP^{+}$ AML population was sorted by fluorescence-activated cell sorting. To KO ICAM-1, sgRNA sequence (CAACTTGGGCTGGTCACAGG) were cloned into the lentiGuide-Puro vectors, as previously described (24,27). The sequences were kindly provided by Dr. Hansen He's laboratory. Lentiviral particles were generated in HEK293T cells using pMDG.2 and psPAX2 packaging plasmids. OCI-AML2 cells were transduced with lentiviral particles for 48 hours, followed by puromycin selection for 72 hours at 1 μg/mL.

Real-time PCR

RNAs from AML cells were isolated using RNeasy Mini Kits (Qiagen), and cDNA was synthesized from the isolated mRNA using QuantiTect Reverse Transcription Kit (Qiagen) in accordance with the manufacturer protocols. Real-time PCR was performed on the LightCycler 480 Instrument (Roche) using the LightCycler 480 SYBR Green I Master (Roche). Results were analyzed using the LightCycler 480 Software version 1.5. Primers for qPCR (Supplementary Table S5) were obtained from Integrated DNA Technologies. RNA expression was normalized to *HPRT* housekeeping gene.

Bulk RNA-sequencing

Total RNA from control and SOCS1 overexpressed OCI-AML2 cells were isolated using RNeasy Mini Kits (Qiagen), and cDNA was synthesized from the isolated mRNA using QuantiTect Reverse Transcription Kit (Qiagen) in accordance with the manufacturer protocols. RNA-sequencing libraries were prepared using Illumina Stranded Total RNA prep (ligation with Ribo-zero Plus kit). Libraries were sequenced as 150-bp paired-end reads in duplicates at ~50 million reads per library using Novaseq 6000 platform at the Princess Margaret Genomic Centre. Four samples were sequenced in total: two replicates for control OCI-AML2 and 2 replicates for SOCS1^{OE} OCI-AML2 groups.

Transcript abundance was quantified from RNA-sequencing reads using Salmon (version 1.4.0). Trimmed sequences were mapped to the human reference genome (GENCODE GRCh38; RRID: SCR_014966) using STAR (RRID:SCR_004463). Salmon quant.sf files were converted into a count matrix for subsequent gene-level analysis using the tximport pipeline (RRID: SCR_016752; version 1.30.0). Differential gene expression analysis between control and SOCS1-overexpressed OCI-AML2 AML cells was performed using DESeq2 package (RRID: SCR_000154) in R (version 4.3.1; RRID: SCR_001905). Gene set enrichment analysis was performed using the clusterProfiler package (RRID: SCR_016884) and Gene Ontology (GO) gene sets provided by MSigDB (https://www.gsea-msigdb.org/gsea/msigdb/) in R.

Patient cohort analyses

The Princess Margaret Cancer Centre cohort encompasses 290 BM samples from adult patients with newly diagnosed, non-promyelocytic AML. NanoString profiling data and clinical annotation (such as T-cell signatures) were retrieved from a prior publication (34) and are accessible through GEO Series (GSE134589). The Cancer Genome Atlas RNA-sequencing data (162 adult AML patients with complete cytogenetic, immunophenotypic and clinical annotation)

were downloaded from cBioPortal (http://www.cbioportal.org/). Survminer package (RRID: SCR_021094) in R was used to plot the Kaplan-Meier curves.

Single-cell RNA-sequencing (scRNA-seq analyses

ScRNA-seq data by Lasry *et al.* (36) (n = 42 patients with newly diagnosed AML) were retrieved from the Gene Expression Omnibus (GEO; RRID: SCR_005012) repository under GEO accession no. GSE185381. After quality control filtering and downstream analysis in Seurat (version 5.0), cells were re-annotated using a curated atlas of BM hematopoiesis with balanced representation of hematopoietic stem and progenitor cells as well as differentiated cells (n = 263,159; BoneMarrowMap package in R). BoneMarrowMap (bioRxiv 2023.12.26.573390) is a large-scale, granular reference atlas of human hematopoiesis, encompassing stem/progenitor cell populations as well as terminally differentiated populations, leveraging a K-Nearest Neighbors classifier to predict leukemic states and providing an unbiased annotation approach. The authors are grateful to Dr. Andy G.X. Zeng and Dr. John Dick (Princess Margaret Cancer Centre, Toronto, Canada) for granting early access to the reference map. Cellular interactions in $SOCS1^{low}$ and $SOCS1^{high}$ BM cells, stratified by median SOCS1 expression across the scRNA-seq dataset, were modeled *in silico* using the CellChat2 package (RRID: SCR_021946) in R with default settings after selecting HSCs as sender and immune effectors ($CD4^+$, $CD8^+$, and NK) as receiver cell populations.

Xenograft model

NOD.Cg-*Prkdc*^{scid}*Il2rg*^{tm1Wjl}*/SzJ* (NSG; RRID: BCBC_4611) mice (Jackson Laboratories) were used for all xenograft experiments and maintained by UHN animal facility. 8-12 week-old female mice were sublethally irradiated (225 cGy) one day prior to an intravenous injection of $1.5x10^6$ MV4-11 or $3x10^6$ cells KG-1a cells. $2x10^7$ DNTs were intravenously

injected on days 3 and 7 for the MV4-11 model and days 14, 17, and 20 for the KG-1a model. 10^4 IU rIL-2 (PROLEUKIN) was given intravenously at the time of DNT infusion and intraperitoneally one week after the last DNT infusion. Mice were euthanized two weeks after the last DNT infusion. BM cells from mice were collected by surgically removing the left femur and flushing the BM contents with a 25G needle and FBS-supplemented RPMI. Next, the BM engraftment level of AML cells were assessed and analyzed using flow cytometry (Supplementary Fig. S33).

Statistical analysis

All graphs and statistical analyses were generated using GraphPad Prism 5 (RRID: SCR_002798) and R. Log-rank test, Wilcoxon signed-rank test, Student's *t*-test, ANOVA, Fisher's exact test, and linear regression tests were used where applicable. ns = nonsignificant, * $p < 0.05$, ** $p < 0.01$, *** $p < 0.001$ indicate statistical significance between groups. Error bars represent ± SEM or ± SD.

Human samples and study approval

Human blood was collected from healthy adult donors and AML patients with written informed consent in accordance with UHN Research Ethics Board (05-0221-T). Animal use was approved by UHN Animal Care Committee (AUP: 741) and experiments were performed according to the Canadian Council on Animal Care Guidelines.

Data availability statement

The data generated in this study are available within the article and its supplementary data files. Bulk RNA sequencing data is publicly available at 10.5281/zenodo.14635075. All other original data generated in this study are available upon reasonable request from the corresponding author(s).

Acknowledgments:

We thank all donors and patients that participated in this study. We also thank the Leukemia Tissue Bank (Princess Margaret Cancer Centre) for providing primary AML patient samples.

Funding:

Canadian Cancer Society Impact Grant (grant #704121) (LZ)
Canadian Institutes of Health Research (grant #419699) (LZ)

Author contributions:

ET, SR, JBL, and LZ conceived and designed the study experiments. ET, SR, JV, IK, YY, NM, YN, and JBL conducted experiments. MDM provided primary patient samples. ET and SR prepared the manuscript. JBL, IK, SR, MDM, NM, YY, ADS, and LZ provided feedback and edited the manuscript.

Conceptualization: ET, SR, JBL, LZ

Methodology: ET, SR, JV, IK, YY, NM, YN, ADS, MDM, and JBL

Investigation: ET, SR, JV, IK, YY, NM, YN, and JBL

Visualization: ET, SR

Funding acquisition: LZ

Supervision: JBL, LZ, ADS

Writing – original draft: ET

Writing – review & editing: JBL, IK, SR, MDM, NM, YY, ADS, and LZ

References

1. DiNardo CD, Jonas BA, Pullarkat V, Thirman MJ, Garcia JS, Wei AH, et al. Azacitidine and Venetoclax in Previously Untreated Acute Myeloid Leukemia. N Engl J Med [Internet]. N Engl J Med; 2020 [cited 2024 May 8];383:617–29. Available from: https://www.nejm.org/doi/full/10.1056/NEJMoa2012971

2. Döhner H, Weisdorf DJ, Bloomfield CD. Acute Myeloid Leukemia. Longo DL, editor. N Engl J Med [Internet]. Massachusetts Medical Society; 2015 [cited 2021 Mar 6];373:1136–52. Available from: http://www.nejm.org/doi/10.1056/NEJMra1406184

3. Lee JB, Chen B, Vasic D, Law AD, Zhang L. Cellular immunotherapy for acute myeloid leukemia: How specific should it be? Blood Rev [Internet]. Elsevier; 2019 [cited 2021 Mar 7];35:18–31. Available from: https://pubmed.ncbi.nlm.nih.gov/30826141/

4. NCI. CAR T Cells: Engineering Immune Cells to Treat Cancer - NCI [Internet]. 2022 [cited 2023 Feb 11]. Available from: https://www.cancer.gov/about-cancer/treatment/research/car-t-cells

5. Cappell KM, Kochenderfer JN. Long-term outcomes following CAR T cell therapy: what we know so far. Nat Rev Clin Oncol [Internet]. Nature Publishing Group; 2023 [cited 2024 Jun 26];20:359–71. Available from: https://www.nature.com/articles/s41571-023-00754-1

6. Sauerer T, Velázquez GF, Schmid C. Relapse of acute myeloid leukemia after allogeneic stem cell transplantation: immune escape mechanisms and current implications for therapy. Mol Cancer [Internet]. BioMed Central; 2023 [cited 2024 Apr 21];22:1–22. Available from: https://molecular-cancer.biomedcentral.com/articles/10.1186/s12943-023-01889-6

7. Hegde PS, Chen DS. Top 10 Challenges in Cancer Immunotherapy. Immunity [Internet]. Elsevier; 2020 [cited 2024 Apr 3];52:17–35. Available from: http://www.cell.com/article/S1074761319305308/fulltext

8. Chen DS, Mellman I. Elements of cancer immunity and the cancer–immune set point. Nat [Internet]. Nature Publishing Group; 2017 [cited 2024 Apr 21];541:321–30. Available from: https://www.nature.com/articles/nature21349

9. Lee JB, Minden MD, Chen WC, Streck E, Chen B, Kang H, et al. Allogeneic human double negative t cells as a novel immunotherapy for acute myeloid leukemia and its underlying mechanisms. Clin Cancer Res [Internet]. 2018 [cited 2023 Jan 22];24:370–82. Available from: https://pubmed.ncbi.nlm.nih.gov/29074605/

10. Lee JB, Kang H, Fang L, D'Souza C, Adeyi O, Zhang L. Developing allogeneic double-negative T cells as a novel off-the-shelf adoptive cellular therapy for cancer. Clin Cancer Res [Internet]. Clin Cancer Res; 2019 [cited 2023 Jan 22];25:2241–53. Available from: https://pubmed.ncbi.nlm.nih.gov/30617140/

11. Tang B, Lee JB, Cheng S, Pan T, Yao W, Wang D, et al. Allogeneic double-negative T cell therapy for relapsed acute myeloid leukemia patients post allogeneic hematopoietic stem cell transplantation: A first-in-human phase I study. Am J Hematol [Internet]. 2022 [cited 2022 Jun 18];97:E264–7. Available from: https://onlinelibrary.wiley.com/doi/full/10.1002/ajh.26564

12. Hu X, li J, Fu M, Zhao X, Wang W. The JAK/STAT signaling pathway: from bench to clinic. Signal Transduct Target Ther [Internet]. Nature Publishing Group; 2021 [cited 2022 Jul 14];6:1–33. Available from: https://www.nature.com/articles/s41392-021-00791-1

13. Shuai K, Liu B. Regulation of JAK–STAT signalling in the immune system. Nat Rev Immunol 2003 311 [Internet]. Nature Publishing Group; 2003 [cited 2021 Dec 21];3:900–11. Available from: https://www.nature.com/articles/nri1226

14. Liau NPD, Laktyushin A, Lucet IS, Murphy JM, Yao S, Whitlock E, et al. The molecular basis of JAK/STAT inhibition by SOCS1. Nat Commun [Internet]. Nature Publishing Group; 2018 [cited 2023 Aug 28];9:1–14. Available from: https://www.nature.com/articles/s41467-018-04013-1

15. Yoshikawa H, Matsubara K, Qian G-S, Jackson P, Groopman JD, Manning JE, et al. SOCS-1, a negative regulator of the JAK/STAT pathway, is silenced by methylation in human hepatocellular carcinoma and shows growth-suppression activity. Nat Genet [Internet]. Nat Genet; 2001 [cited 2024 Mar 26];28:29–35. Available from: https://pubmed.ncbi.nlm.nih.gov/11326271/

16. Zhang XH, Yang L, Liu XJ, Zhan Y, Pan YX, Wang XZ, et al. Association between methylation of tumor suppressor gene SOCS1 and acute myeloid leukemia. Oncol Rep [Internet]. Oncol Rep; 2018 [cited 2024 Mar 26];40:1008–16. Available from: https://pubmed.ncbi.nlm.nih.gov/29916533/

17. Hou HA, Lu JW, Lin TY, Tsai CH, Chou WC, Lin CC, et al. Clinico-biological significance of suppressor of cytokine signaling 1 expression in acute myeloid leukemia. Blood Cancer J [Internet]. Nature Publishing Group; 2017 [cited 2022 Dec 17];7:e588. Available from: https://pubmed.ncbi.nlm.nih.gov/28753595/

18. Reddy PNG, Sargin B, Choudhary C, Stein S, Grez M, Müller-Tidow C, et al. SOCS1 cooperates with FLT3-ITD in the development of myeloproliferative disease by promoting the escape from external cytokine control. Blood. Content Repository Only!; 2012;120:1691–702.

19. Liang D, Wang Q, Zhang W, Tang H, Song C, Yan Z, et al. JAK/STAT in leukemia: a clinical update. Mol Cancer [Internet]. BioMed Central Ltd; 2024 [cited 2024 Mar 26];23:1–12. Available from: https://molecular-cancer.biomedcentral.com/articles/10.1186/s12943-023-01929-1

20. Zeidan AM, Cook RJ, Bordoni R, Berenson JR, Edenfield WJ, Mohan S, et al. A Phase 1/2 Study of the Oral Janus Kinase 1 Inhibitors INCB052793 and Itacitinib Alone or in Combination With Standard Therapies for Advanced Hematologic Malignancies. Clin Lymphoma Myeloma Leuk [Internet]. Clin Lymphoma Myeloma Leuk; 2022 [cited 2022 Sep 12];22:523–34. Available from: https://pubmed.ncbi.nlm.nih.gov/35260349/

21. Pemmaraju N, Kantarjian H, Kadia T, Cortes J, Borthakur G, Newberry K, et al. A Phase I/II Study of the Janus Kinase (JAK)1 and 2 Inhibitor Ruxolitinib in Patients with Relapsed or Refractory Acute Myeloid Leukemia. Clin Lymphoma Myeloma Leuk [Internet]. NIH Public Access; 2015 [cited 2021 Oct 31];15:171. Available from: /pmc/articles/PMC4344906/

22. Eghtedar A, Verstovsek S, Estrov Z, Burger J, Cortes J, Bivins C, et al. Phase 2 study of the JAK kinase inhibitor ruxolitinib in patients with refractory leukemias, including postmyeloproliferative neoplasm acute myeloid leukemia. Blood [Internet]. 2012 [cited 2022 Oct 26];119:4614–8. Available from: https://pubmed.ncbi.nlm.nih.gov/22422826/

23. Lee JB, Khan DH, Hurren R, Xu M, Na Y, Kang H, et al. Venetoclax enhances T cell–mediated antileukemic activity by increasing ROS production. Blood [Internet]. American Society of Hematology; 2021 [cited 2024 Mar 26];138:234–45. Available from: https://dx.doi.org/10.1182/blood.2020009081

24. Soares F, Chen B, Lee JB, Ahmed M, Ly D, Tin E, et al. CRISPR screen identifies genes that sensitize AML cells to double-negative T-cell therapy. Blood [Internet]. Blood; 2021 [cited 2023 Jan 22];137:2171–81. Available from: https://pubmed.ncbi.nlm.nih.gov/33270841/

25. Lurie RH, Platanias LC. Mechanisms of type-I- and type-II-interferon-mediated signalling. Nat Rev Immunol [Internet]. Nature Publishing Group; 2005 [cited 2024 Mar 26];5:375–86. Available from: https://www.nature.com/articles/nri1604

26. Miscia S, Marchisio M, Grilli A, Di Valerio V, Centurione L, Sabatino G, et al. Tumor necrosis factor α (TNF-α) activates Jak1/Stat3-Stat5b signaling through TNFR-1 in human B cells. Cell Growth Differ. 2002;13:13–8.

27. Tin E, Lee JB, Khatri I, Na Y, Minden MD, Zhang L. Double-negative T cells utilize a TNFα–JAK1–ICAM-1 cytotoxic axis against acute myeloid leukemia. Blood Adv [Internet]. American Society of Hematology; 2024 [cited 2024 Apr 6];8:3013–26. Available from: https://dx.doi.org/10.1182/bloodadvances.2023011739

28. Sayitoglu EC, Luca BA, Boss AP, Thomas BC, Freeborn RA, Uyeda MJ, et al. AML/T cell interactomics uncover correlates of patient outcomes and the key role of ICAM1 in T cell killing of AML. Leuk 2024 [Internet]. Nature Publishing Group; 2024 [cited 2024 May 13];1–10. Available from: https://www.nature.com/articles/s41375-024-02255-1

29. Lötscher J, Martí i Líndez AA, Kirchhammer N, Cribioli E, Giordano Attianese GMP, Trefny MP, et al. Magnesium sensing via LFA-1 regulates CD8+ T cell effector function. Cell. 2022;185:585-602.e29.

30. Wang MS, Hu Y, Sanchez EE, Xie X, Roy NH, de Jesus M, et al. Mechanically active integrins target lytic secretion at the immune synapse to facilitate cellular cytotoxicity. Nat Commun [Internet]. Nat Commun; 2022 [cited 2022 Jun 18];13:3222. Available from: https://pubmed.ncbi.nlm.nih.gov/35680882/

31. Petit AE, Demotte N, Scheid B, Wildmann C, Bigirimana R, Gordon-Alonso M, et al. A major secretory defect of tumour-infiltrating T lymphocytes due to galectin impairing LFA-1-mediated synapse completion. Nat Commun [Internet]. Nat Commun; 2016 [cited 2024 Oct 23];7. Available from: https://pubmed.ncbi.nlm.nih.gov/27447355/

32. Reina M, Espel E. Role of LFA-1 and ICAM-1 in Cancer. Cancers 2017, Vol 9, Page 153 [Internet]. Multidisciplinary Digital Publishing Institute; 2017 [cited 2024 Mar 26];9:153. Available from: https://www.mdpi.com/2072-6694/9/11/153/htm

33. Wang B, Reville PK, Yassouf MY, Jelloul FZ, Ly C, Desai PN, et al. Comprehensive characterization of IFNγ signaling in acute myeloid leukemia reveals prognostic and

therapeutic strategies. Nat Commun [Internet]. Nature Publishing Group; 2024 [cited 2024 Nov 7];15:1–16. Available from: https://www.nature.com/articles/s41467-024-45916-6

34. Vadakekolathu J, Minden MD, Hood T, Church SE, Reeder S, Altmann H, et al. Immune landscapes predict chemotherapy resistance and immunotherapy response in acute myeloid leukemia. Sci Transl Med [Internet]. American Association for the Advancement of Science; 2020 [cited 2024 Mar 26];12:463. Available from: https://www.science.org/doi/10.1126/scitranslmed.aaz0463

35. Christopher MJ, Petti AA, Rettig MP, Miller CA, Chendamarai E, Duncavage EJ, et al. Immune Escape of Relapsed AML Cells after Allogeneic Transplantation. N Engl J Med [Internet]. Massachusetts Medical Society; 2018 [cited 2024 May 21];379:2330–41. Available from: https://www.nejm.org/doi/full/10.1056/NEJMoa1808777

36. Lasry A, Nadorp B, Fornerod M, Nicolet D, Wu H, Walker CJ, et al. An inflammatory state remodels the immune microenvironment and improves risk stratification in acute myeloid leukemia. Nat cancer [Internet]. Nat Cancer; 2023 [cited 2024 May 20];4:27–42. Available from: https://pubmed.ncbi.nlm.nih.gov/36581735/

37. Pan D, Kobayashi A, Jiang P, De Andrade LF, Tay RE, Luoma AM, et al. A major chromatin regulator determines resistance of tumor cells to T cell-mediated killing. Science [Internet]. Science; 2018 [cited 2024 Apr 22];359:770–5. Available from: https://pubmed.ncbi.nlm.nih.gov/29301958/

38. Lawson KA, Sousa CM, Zhang X, Kim E, Akthar R, Caumanns JJ, et al. Functional genomic landscape of cancer-intrinsic evasion of killing by T cells. Nature [Internet]. NIH Public Access; 2020 [cited 2023 May 27];586:120. Available from: /pmc/articles/PMC9014559/

39. Ramos A, Koch CE, Liu-Lupo Y, Hellinger RD, Kyung T, Abbott KL, et al. Leukemia-intrinsic determinants of CAR-T response revealed by iterative in vivo genome-wide CRISPR screening. Nat Commun [Internet]. Nature Publishing Group; 2023 [cited 2024 Apr 12];14:1–21. Available from: https://www.nature.com/articles/s41467-023-43790-2

40. Wu Q-YY, Zhu Y-YY, Liu Y, Wei F, Tong Y-XX, Cao J, et al. CUEDC2, a novel interacting partner of the SOCS1 protein, plays important roles in the leukaemogenesis of acute myeloid leukaemia. Cell Death Dis [Internet]. Nature Publishing Group; 2018 [cited 2021 Oct 31];9. Available from: /pmc/articles/PMC6039501/

41. Lamble AJ, Kosaka Y, Laderas T, Maffit A, Kaempf A, Brady LK, et al. Reversible suppression of T cell function in the bone marrow microenvironment of acute myeloid leukemia. Proc Natl Acad Sci U S A [Internet]. Proc Natl Acad Sci U S A; 2020 [cited 2024 Nov 12];117:14331–41. Available from: https://pubmed.ncbi.nlm.nih.gov/32513686/

42. Mazziotta F, Biavati L, Rimando J, Rutella S, Borcherding N, Parbhoo S, et al. CD8+ T-cell differentiation and dysfunction inform treatment response in acute myeloid leukemia. Blood [Internet]. Blood; 2024 [cited 2024 Nov 12];144:1168–82. Available from: https://pubmed.ncbi.nlm.nih.gov/38776511/

43. Le Dieu R, Taussig DC, Ramsay AG, Mitter R, Miraki-Moud F, Fatah R, et al. Peripheral blood T cells in acute myeloid leukemia (AML) patients at diagnosis have abnormal phenotype and genotype and form defective immune synapses with AML blasts. Blood

[Internet]. Blood; 2009 [cited 2024 May 14];114:3909–16. Available from: https://pubmed.ncbi.nlm.nih.gov/19710498/

44. Kantari-Mimoun C, Barrin S, Vimeux L, Haghiri S, Gervais C, Joaquina S, et al. CAR T-cell Entry into Tumor Islets Is a Two-Step Process Dependent on IFNγ and ICAM-1. Cancer Immunol Res [Internet]. Cancer Immunol Res; 2021 [cited 2024 Mar 26];9:1425–38. Available from: https://pubmed.ncbi.nlm.nih.gov/34686489/

45. Vasic D, Lee JB, Leung Y, Khatri I, Na Y, Abate-Daga D, et al. Allogeneic double-negative CAR-T cells inhibit tumor growth without off-tumor toxicities. Sci Immunol [Internet]. American Association for the Advancement of Science; 2022 [cited 2024 Mar 26];7:3642. Available from: https://www.science.org/doi/10.1126/sciimmunol.abl3642

46. Fang KKL, Lee J, Khatri I, Na Y, Zhang L. Targeting T-cell malignancies using allogeneic double-negative CD4-CAR-T cells. J Immunother cancer [Internet]. J Immunother Cancer; 2023 [cited 2024 Mar 26];11. Available from: https://pubmed.ncbi.nlm.nih.gov/37678917/

47. Chen WC, Xing Y, Yuan JS, Mitchell A, Mbong N, Popescu AC, et al. An Integrated Analysis of Heterogeneous Drug Responses in Acute Myeloid Leukemia That Enables the Discovery of Predictive Biomarkers. Cancer Res [Internet]. 2016 [cited 2021 Nov 12];76:1214–24. Available from: https://cancerres.aacrjournals.org/content/76/5/1214

48. Song C, Liu D, Liu S, Li D, Horecny I, Zhang X, et al. SHR1032, a novel STING agonist, stimulates anti-tumor immunity and directly induces AML apoptosis. Sci Reports 2022 121 [Internet]. Sci Rep; 2022 [cited 2022 Nov 30];12:1–12. Available from: https://www.nature.com/articles/s41598-022-12449-1

49. Zhu Y, An X, Zhang X, Qiao Y, Zheng T, Li X. STING: a master regulator in the cancer-immunity cycle. Mol Cancer [Internet]. BioMed Central; 2019 [cited 2022 Dec 14];18:1–15. Available from: https://molecular-cancer.biomedcentral.com/articles/10.1186/s12943-019-1087-y

50. Hart T, Chandrashekhar M, Aregger M, Steinhart Z, Brown KR, MacLeod G, et al. High-Resolution CRISPR Screens Reveal Fitness Genes and Genotype-Specific Cancer Liabilities. Cell [Internet]. Cell; 2015 [cited 2024 May 8];163:1515–26. Available from: https://pubmed.ncbi.nlm.nih.gov/26627737/

Figure 1. Intrinsic SOCS1 expression level in AML regulates its susceptibility to T-cell killing.

A) Waterfall plot of enriched (susceptibility genes) and depleted (resistance genes) sgRNAs in OCI-AML2 cells after DNT treatment relative to DNT-untreated control from the genome-wide Cas9^{+} OCI-AML2 CRISPR screen. Each dot represents a gene, and y-axis represents relative sgRNA enrichment score determined by NormZ in DNT-treated AML cells relative to the untreated. Genes (black) that are significantly enriched or depleted (FDR $\leq 1x10^{-5}$) and are associated with the SOCS1-JAK1-STAT1 signaling pathway are displayed.

B) Schematic of SOCS1-JAK1-STAT1 signaling pathway based on CRISPR screen hits.(13)

(C and D) **(C)** KG-1a and **(D)** primary AML blast (n=3) silenced with shRNAs against SOCS1 (shSOCS1) or control shRNA were cultured alone or with **(C)** T cells or **(D)** DNTs. 4:1 ratio with multi-day incubation was used for KG-1a and a 24-hour co-incubation with varying ratios were used for primary AML samples. Specific killing of target cells was determined by flow cytometry and DAPI to measure dead cells. Percentage specific killing was calculated by $\frac{\%\ Dead_{with\ T\ cells} - \%\ Dead_{without\ T\ cells}}{100 - \%\ Dead_{without\ T\ cells}}$ x 100%. Experiments were done with technical triplicates or duplicates and were performed with at least two DNT donors. Representative data are shown. Numbers represent the AML patient ID, and error bars represent SEM. Two-way ANOVA was used for statistics. * $p < 0.05$, ** $p < 0.01$, *** $p < 0.001$.

(E and F) Sublethally irradiated (225 cGy) NSG mice were intravenously injected with control or SOCS1-silenced KG-1a, followed by three infusions of DNTs or PBS. **(E)** The treatment schedule of the *in vivo* xenograft mouse model is shown. Bar graphs represent

the mean AML BM engraftment levels pooled from two independent experiments (n=6-8/group) of **(F)** control KG-1a-infused mice (left) and SOCS1-silenced KG-1a-infused mice (right) with or without DNT infusions. Each symbol represents the AML engraftment for an individual mouse. Error bars represent SD. Student's *t*-test was used for statistics. ns = nonsignificant, * $p < 0.05$.

G) Control or SOCS1-overexpressed (SOCS1 OE) AML cell lines (OCI-AML2 and MV4-11) were co-cultured with DNTs or T_{conv} cells at 0.25:1 or 4:1 ratio, respectively. Percentage specific killing by T cells was determined by flow cytometry. The experiment was performed with technical triplicates, and the data shown are representative of three independent experiments. Errors bars represent SD. Two-way ANOVA was used for statistics. *** $p < 0.001$.

(H and I) Sublethally irradiated (225 cGy) NSG mice were intravenously injected with control or SOCS1-overexpressed MV4-11, followed by two infusions of DNTs or PBS. **(H)** Treatment schedule of the *in vivo* xenograft mouse model is shown. Bar graphs represent the mean AML BM engraftment levels pooled from two independent experiments (n=6-10/group) of **(I)** control MV4-11-infused mice (left) and SOCS1-overexpressed MV4-11-infused mice (right) with or without DNT infusions. Each symbol represents the AML engraftment for an individual mouse. Error bars represent SD. Student's *t*-test was used for statistics. ns = nonsignificant, ** $p < 0.01$.

J) Correlation between *SOCS1* expression in AML cell lines (n=4) and primary AML blasts (n=6) determined by qPCR and DNT-specific killing at 2:1 ratio measured by flow cytometry. Each symbol represents an AML cell line or a primary AML sample. Numbers represent the AML patient ID. Experiments were done with technical duplicates

or triplicates and performed with at least two DNT donors. Representative data are shown. Error bars represent SEM. Linear regression test was used for statistics.

Figure 2. **JAK1 activity, but not expression level, correlates with AML resistance to T-cell immunity**.

A) Control and JAK1-silenced (shJAK1) AML cell lines (OCI-AML2 and MV4-11) were co-incubated with T cells for 24 hours (DNTs, 0.25:1 ratio; T_{conv} cells, 4:1 ratio). Viability of AML cells were measured by flow cytometry. Experiments were done with technical triplicates. The graphs shown are representative of two independent experiments. Error bars represent SD. Two-way ANOVA was used for statistics. *** $p < 0.001$.

(B and C) (B) AML cell lines (OCI-AML2, OCI-AML3, and MV4-11) and **(C)** primary AML blasts (150549, 100753, 140176, 130794, and 100857) were pre-treated for 24 hours or treated with a JAK1-inhibitor, itacitinib (10 μM), respectively, or DMSO as controls. Subsequently, the cells were co-cultured with **(B)** T_{conv} cells or **(B and C)** DNTs for 24 hours. Percentage specific killing was calculated by Annexin-V staining via flow cytometry. Experiments were done with technical triplicates or duplicates and performed with at least two T cell donors. Representative data are shown. Error bars represent **(B)** SD and **(C)** SEM. Two-way ANOVA was used for statistics. *** $p < 0.001$.

(D and E) Sublethally irradiated (225 cGy) NSG mice were intravenously injected with control or JAK1-silenced MV4-11, followed by two DNT injections. Bar graphs represent the mean AML BM engraftment levels pooled from three independent experiments (n=10-14/group) of **(D)** control MV4-11-infused mice (left) and JAK1-silenced MV4-11-infused mice (right) with or without DNT infusions. Each symbol

represents AML engraftment in individual mouse. Error bars represent the SD. Student's *t*-test was used for statistics. ns = nonsignificant, * $p < 0.05$. **(E)** Viable AML cells from mouse femurs were harvested and co-cultured with DNTs *ex vivo* for 24 hours. Percentage specific killing was determined by flow cytometry. Error bars represent SEM. Two-way ANOVA was used for statistics. *** $p < 0.001$.

F) AML cells were cultured with or without DNTs at a 0.5:1 ratio for 2 hours. The correlation between the mean fluorescence intensity (MFI) fold change of pSTAT1 expression in AML post co-culture with DNTs and DNT-specific killing measured by flow cytometry was determined by linear regression. Each symbol represents an AML cell line or primary AML sample. Numbers represent the AML patient ID. Experiments were done with technical duplicates and performed with at least two DNT donors. Representative data are shown. Linear regression test was used for statistics. Error bars represent SEM.

Figure 3. **T-cell effector function against AML is dependent on the SOCS1-JAK1 axis.**

(A and B) (A) SOCS1-overexpressed (SOCS1 OE) AML cells and **(B)** SOCS1-silenced (shSOCS1) KG-1a cells were cultured with or without DNTs at 0.5:1 ratio and intracellularly stained for pSTAT1. The pSTAT1 expression level was determined by flow cytometry. Experiments were performed with technical duplicates, and the data are representative of two independent experiments. One-way ANOVA was used for statistics. Error bars represent SD. ns = nonsignificant, ** $p < 0.01$, *** $p < 0.001$.

C) Expression of intracellular pSTAT1 in control or SOCS1-overexpressed (SOCS1 OE) OCI-AML2 cells treated with varying concentrations of rIFNγ for 24 hours. MFI values of pSTAT1 detected by flow cytometry is shown. Data shown are representative of two

independent experiments performed with technical duplicates. Error bars represent SEM. Two-way ANOVA was used for statistics. ** $p < 0.01$, *** $p < 0.001$.

D) Control and SOCS1-overexpressed OCI-AML2 cells were stimulated with varying concentrations of rIFNγ for 24 hours, washed, then co-cultured with DNTs at 1:1 ratio or T_{conv} cells at 4:1 ratio for 2 hours. Percentage specific killing was determined by flow cytometry. Data shown are representative of two independent experiments, and experiments were performed with technical triplicates. Error bars represent SEM. Two-way ANOVA was used for statistics. ** $p < 0.01$, *** $p < 0.001$.

E) Control and SOCS1-silenced (shSOCS1) AML cells were pre-treated with or without rIFNγ (50 ηg/mL), washed, then co-cultured with DNTs at 4:1 (for KG-1a) and 2:1 (for primary AML) E:T ratios. Percentage increase in specific killing was calculated by comparing treated and untreated groups. Experiments were performed with technical triplicates or duplicates with at least two DNT donors. Representative data are shown. Error bars represent SD. Student's *t*-test was used for statistics. * $p < 0.05$, ** $p < 0.01$.

F) AML cell lines (n=4) and primary AML blasts (n=4) were treated with or without rIFNγ (50 ηg/mL), washed, then co-cultured with DNTs. Linear regression was performed between percentage increase in specific killing measured by flow cytometry and SOCS1 expression levels detected by qPCR. Each symbol represents an AML cell line or primary AML sample. Numbers represent the AML patient ID. Experiments were done with technical duplicates and performed with at least two DNT donors. Representative data are shown. Error bars represent SEM. Linear regression test was used for statistics.

Figure 4. ICAM-1 is crucial for the SOCS1-JAK1 axis to alter AML sensitivity to T-cell killing.

A) Control and SOCS1-overexpressed OCI-AML2 cells were stimulated with or without rIFNγ (50 ηg/mL) and stained for various markers. MFI fold change of molecules on untreated and treated AML cells was determined with flow cytometry. Graph shown is representative of two independent experiments.

(B and C) (B) SOCS1-overexpressed AML cell lines, **(C)** SOCS1-silenced KG-1a, and control AML cells were co-incubated with DNTs or T_{conv} cells for **(B)** 24 and **(C)** 48 hours. Subsequently, the expression of ICAM-1 on AML cells were determined by flow and MFI fold change between AML cells with or without T cells were calculated. 0.25:1 (DNT) and 2:1 (T_{conv} cell) E:T ratios were used for SOCS1-overexpressed AML, and 4:1 ratio was used for SOCS1-silenced AML. Data are representative of at least two independent experiments, and experiments were performed with technical triplicates. Error bars represent SD. Two-way ANOVA was used for statistics. *** $p < 0.001$.

D) MV4-11 cells harvested from the BM of DNT-treated mice in Figure 1H were stained for ICAM-1. MFI values of ICAM-1 expression on AML cells were measured by flow cytometry. Each symbol represents an individual mouse. Error bars represent SD. The results shown are the summary of two independent experiments (n=6-8/group). Student's *t*-test was used for statistics. *** $p < 0.001$.

E) AML cell lines (n=4) and primary AML blasts (n=8) were treated with or without rIFNγ (50 ηg/mL) for 24 hours. Linear regression was performed between MFI fold change in ICAM-1 with or without rIFNγ treatment determined by flow cytometry and *SOCS1* expression levels detected by qPCR. Each symbol represents an AML cell line or primary

AML sample. Numbers represent the AML patient ID. Experiments were done with technical duplicates. Representative data are shown. Error bars represent SEM. Linear regression test was used for statistics.

F) Control and SOCS1-silenced KG-1a cells were co-cultured with DNTs at a 4:1 E:T ratio for two days, in the presence of ICAM-1 neutralizing antibody (5 µg/mL) or isotype control. Specific killing and increase in specific killing between control and SOCS1-silenced AML cells were determined by flow cytometry. Experiments were performed with technical triplicates. Graphs shown are representative of two independent experiments. Error bars represent SD. One-way ANOVA (left) and Student's *t*-test (right) were used for statistics. *** $p < 0.001$.

G) Control and ICAM-1^{KO} OCI-AML2 cells were treated with or without rIFNγ (50 ηg/mL), washed, then co-incubated with DNTs at a 1:1 E:T ratio. Percentage increase in specific killing between untreated and treated AML cells was determined by flow cytometry. Data shown are representative of two independent experiments performed with technical duplicates. Error bars represent SD. Student's *t*-test was used for statistics. * $p < 0.05$.

(H and I) AML cells were treated with or without rIFNγ (50 ηg/mL) for 24 hours, washed, then co-incubated with T cells in the presence of ICAM-1 neutralizing antibody (5 µg/mL) or isotype control. **(H)** AML cell lines were co-cultured at 1:1 (for DNTs) and 4:1 (for T_{conv} cells) E:T ratio. **(I)** Primary AML blasts were co-incubated with DNTs at 2:1 E:T ratio. Percentage increase in specific killing following rIFNγ treatment was determined by flow cytometry. Experiments were performed with technical triplicates or duplicates with at least two DNT donors. Representative data are shown. Error bars

represent SD. **(H)** Two-way ANOVA and **(I)** Student's *t*-test were used for statistics. ns = nonsignificant, *** $p < 0.001$.

J) AML cells were treated with or without rIFNγ (50 ηg/mL), washed, then co-cultured with DNTs. The correlation between MFI fold change in ICAM-1 and percentage increase in specific killing between untreated and treated AML cells measured by flow cytometry was determined by linear regression. Each symbol represents an AML cell line or primary AML sample. Numbers represent the AML patient ID. Experiments were done with technical duplicates and performed with at least two DNT donors. Representative data are shown. Error bars represent SEM. Linear regression test was used for statistics.

Figure 5. SOCS1 inversely correlates with AML patient survival without affecting disease burden.

(A and B) Kaplan-Meier estimates of overall survival stratified by median SOCS1 expression in AML patients from the **(A)** TCGA-LAML and **(B)** PMCC cohort. Log-rank test was used for statistics.

C) Percentage BM AML blasts (n=175/287, left) and number of AML blasts (n=174/287, right) in patients from the PMCC cohort stratified by median SOCS1 expression. Boxplots are shown. Wilcoxon signed-rank test was used for statistics. ns = nonsignificant.

D) Sublethally irradiated (225 cGy) NSG mice were intravenously injected with SOCS1-silenced KG-1a (left), SOCS1-overexpressed MV4-11 (right), or respective control AML cells. AML cells from the BM of KG-1a-engrafted and MV4-11-engrafted mice were harvested after 35 days and 21 days, respectively. Bar graphs represent the mean AML BM engraftment levels. Each symbol represents the AML engraftment for individual

mouse. Error bars represent SD. The results shown are the summary of two independent experiments (n=8-10/group). Student's *t*-test was used for statistics. ns = nonsignificant.

E) Gene set enrichment analysis was performed on differentially expressed genes (adjusted *p*-value < 0.05) between control and SOCS1-overexpressed OCI-AML2 cells. Top 16 GO gene sets with adjusted *p*-values and normalized enrichment scores are shown. Fisher's exact test was used for statistics.

(F and G) *In silico* modeling of inferred cellular interactions in $SOCS1^{high}$ and $SOCS1^{low}$ BM cells **(F)** overall and **(G)** predicted cross-talk between $CD4^+$ T cells, $CD8^+$ T cells, and HSCs using the Lasry *et al.* AML dataset and CellChat2 in R (36). Green rectangles highlight the interaction between $CD4^+$ T cells and HSCs, and blue rectangles highlight the interaction between $CD8^+$ T cells and HSCs.

H) Kaplan-Meier estimates of overall survival in PMCC patients with low or high SOCS1 expression, determined in Figure 5B, stratified by median exhausted $CD8^+$ T-cell score (34). Log-rank test was used for statistics.

I) Schematic of the SOCS1 pathway to suppress the IFNγ-JAK1-mediated upregulation of ICAM-1 and subsequent T-cell killing of AML.

Figure 1

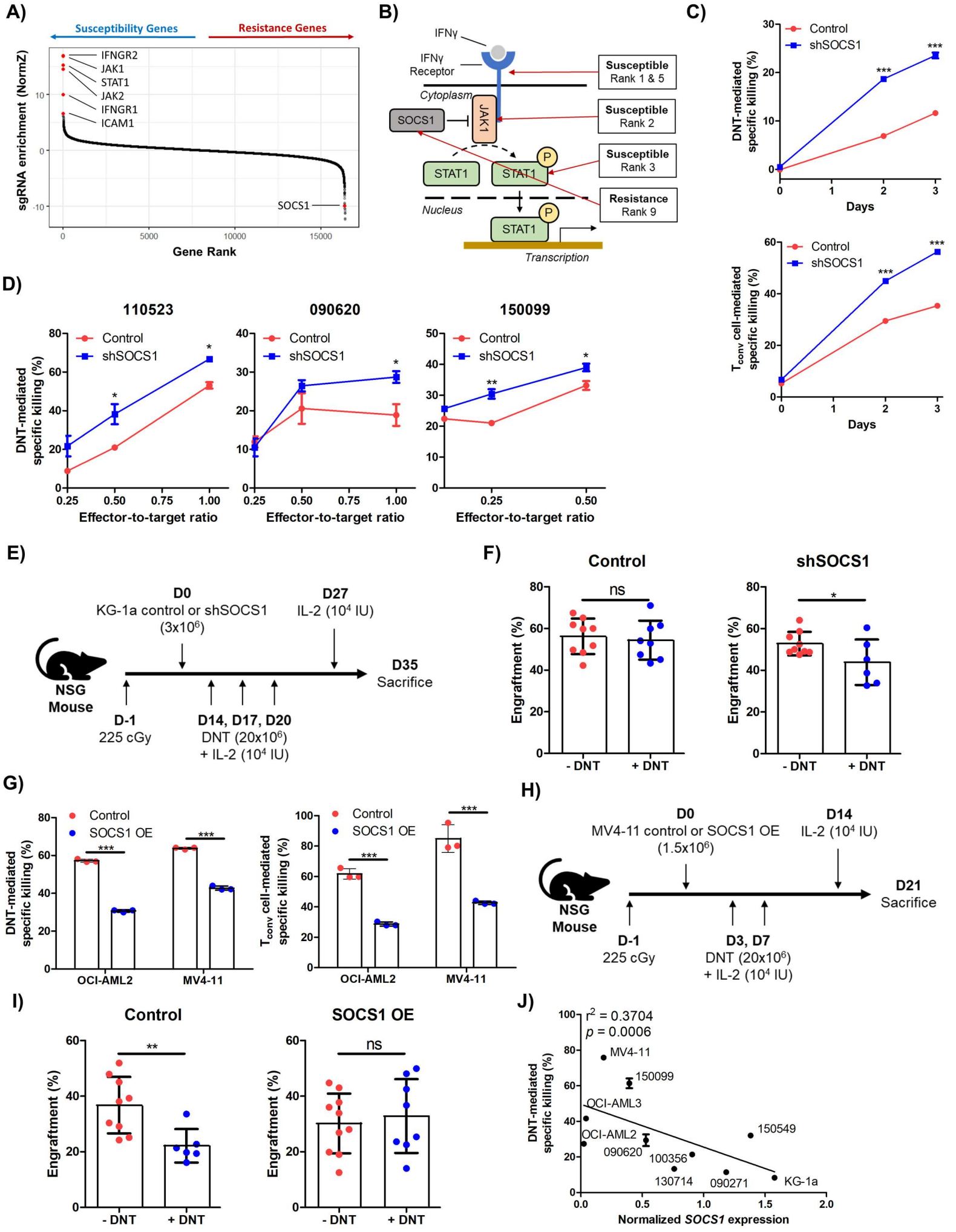
A)
Susceptibility Genes
Resistance Genes
IFNGR2
JAK1
STAT1
JAK2
IFNGR1
ICAM1
SOCS1
sgRNA enrichment (NormZ)
Gene Rank
B)
IFNγ
IFNγ Receptor
Cytoplasm
JAK1
SOCS1
STAT1
STAT1
Nucleus
STAT1
Transcription
Susceptible Rank 1 & 5
Susceptible Rank 2
Susceptible Rank 3
Resistance Rank 9
C)
Control
shSOCS1
DNT-mediated specific killing (%)
Days
Tconv cell-mediated specific killing (%)
D)
110523
090620
150099
Effector-to-target ratio
E)
D0
KG-1a control or shSOCS1 (3x10^6)
D27
IL-2 (10^4 IU)
NSG Mouse
D-1
225 cGy
D14, D17, D20
DNT (20x10^6) + IL-2 (10^4 IU)
D35
Sacrifice
F)
Control
shSOCS1
Engraftment (%)
ns
- DNT
+ DNT
G)
SOCS1 OE
OCI-AML2
MV4-11
H)
D0
MV4-11 control or SOCS1 OE (1.5x10^6)
D14
IL-2 (10^4 IU)
D21
Sacrifice
D3, D7
I)
J)
r^2 = 0.3704
p = 0.0006
MV4-11
150099
OCI-AML3
OCI-AML2
090620
150549
100356
130714
090271
KG-1a
Normalized SOCS1 expression

Figure 2

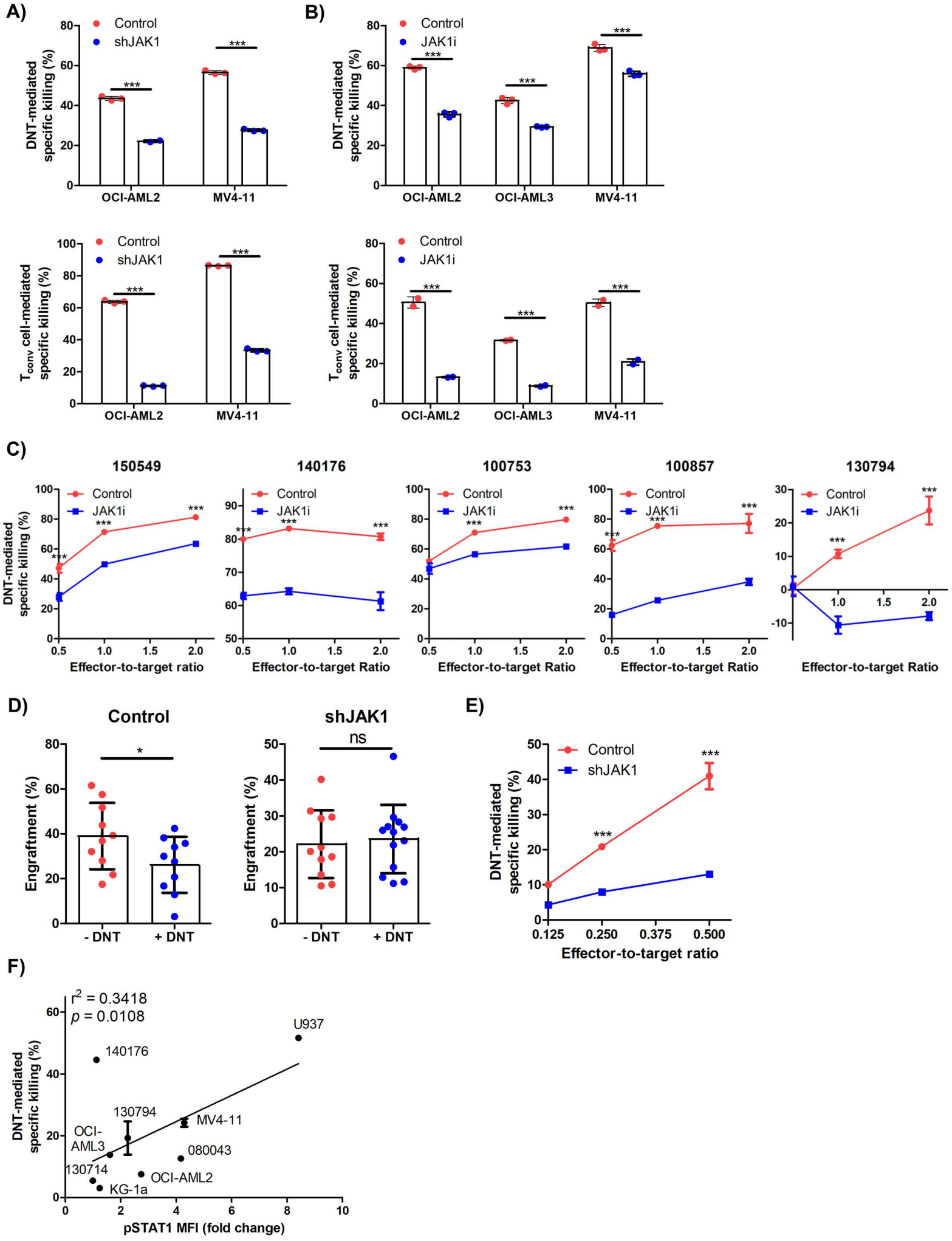
A)
Control
shJAK1
DNT-mediated specific killing (%)
OCI-AML2
MV4-11
B)
Control
JAK1i
DNT-mediated specific killing (%)
OCI-AML2
OCI-AML3
MV4-11
Control
shJAK1
Tconv cell-mediated specific killing (%)
OCI-AML2
MV4-11
Control
JAK1i
Tconv cell-mediated specific killing (%)
OCI-AML2
OCI-AML3
MV4-11
C)
150549
140176
100753
100857
130794
Control
JAK1i
DNT-mediated specific killing (%)
Effector-to-target ratio
Effector-to-target Ratio
D)
Control
shJAK1
ns
Engraftment (%)
- DNT
+ DNT
E)
Control
shJAK1
DNT-mediated specific killing (%)
Effector-to-target ratio
F)
r2 = 0.3418
p = 0.0108
U937
140176
130794
MV4-11
OCI-AML3
080043
130714
OCI-AML2
KG-1a
DNT-mediated specific killing (%)
pSTAT1 MFI (fold change)

Figure 3

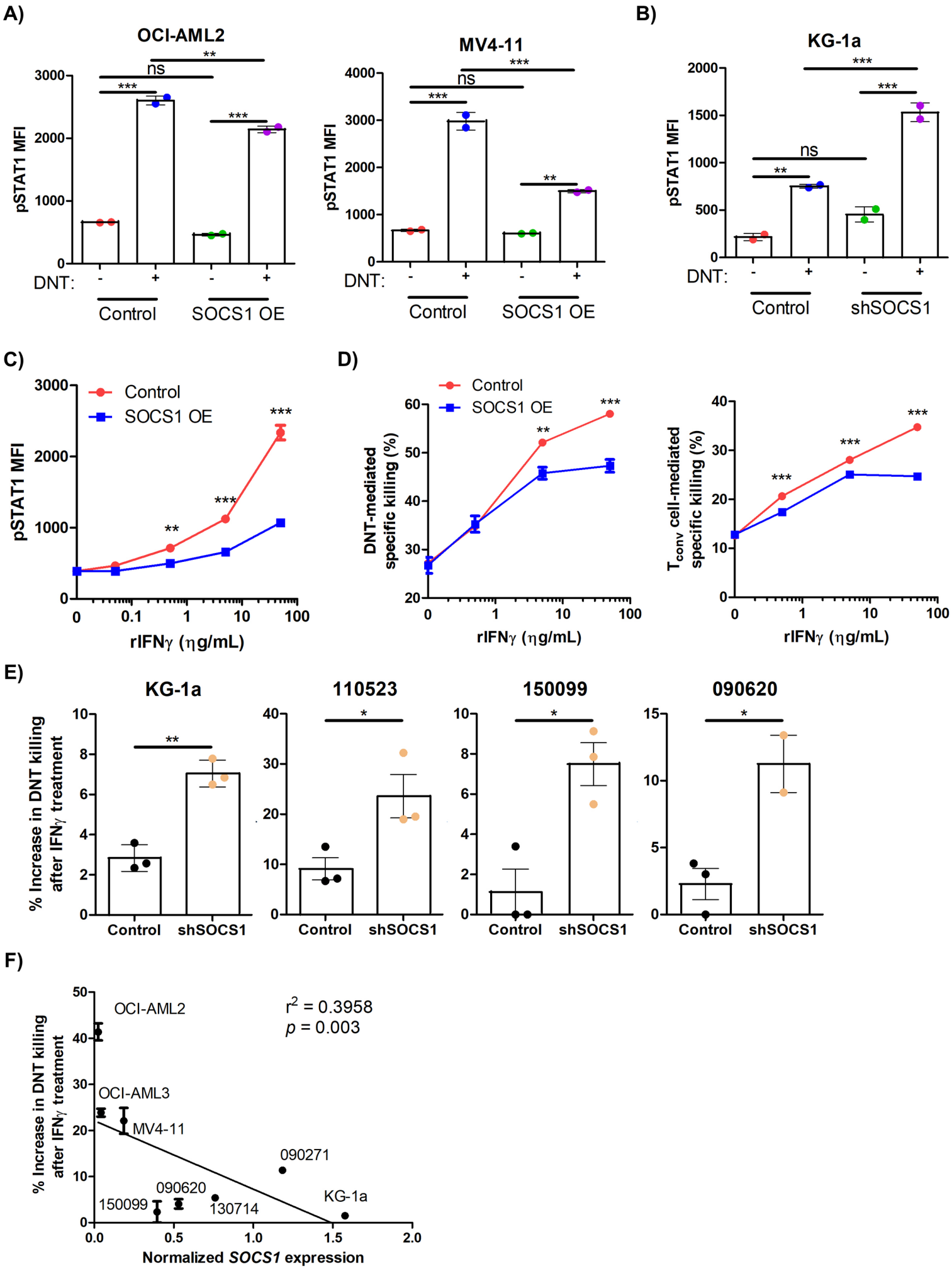
A)
OCI-AML2
MV4-11
pSTAT1 MFI
DNT:
Control
SOCS1 OE
B)
KG-1a
shSOCS1
C)
Control
SOCS1 OE
rIFNγ (ηg/mL)
D)
DNT-mediated specific killing (%)
Tconv cell-mediated specific killing (%)
E)
KG-1a
110523
150099
090620
% Increase in DNT killing after IFNγ treatment
F)
r2 = 0.3958
p = 0.003
OCI-AML2
OCI-AML3
MV4-11
090271
090620
150099
130714
KG-1a
Normalized SOCS1 expression

Figure 4

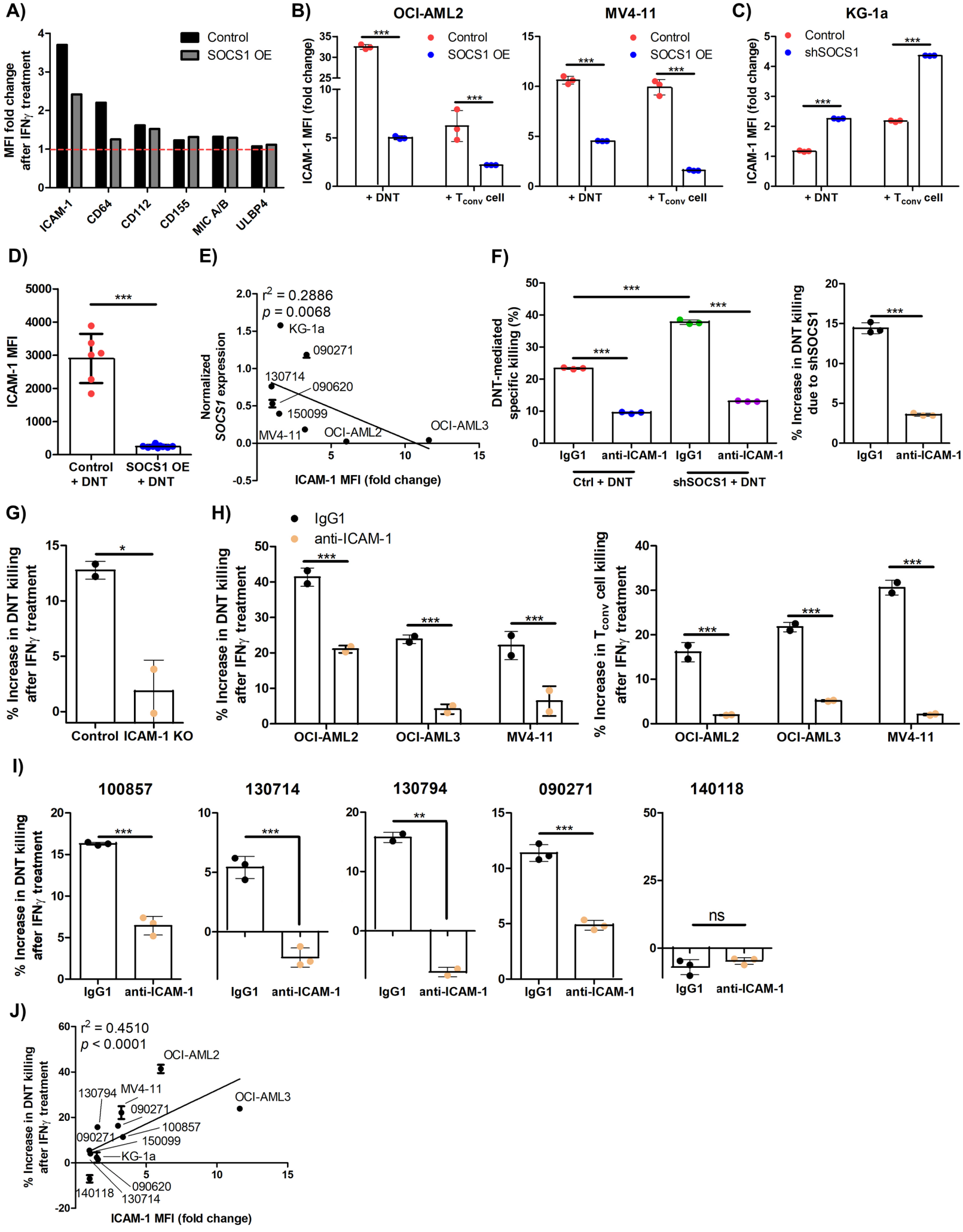
A)
MFI fold change after IFNγ treatment
Control
SOCS1 OE
ICAM-1
CD64
CD112
CD155
MIC A/B
ULBP4
B)
OCI-AML2
MV4-11
ICAM-1 MFI (fold change)
Control
SOCS1 OE
+ DNT
+ Tconv cell
C)
KG-1a
Control
shSOCS1
D)
ICAM-1 MFI
Control + DNT
SOCS1 OE + DNT
E)
r2 = 0.2886
p = 0.0068
Normalized SOCS1 expression
KG-1a
090271
130714
090620
150099
MV4-11
OCI-AML2
OCI-AML3
ICAM-1 MFI (fold change)
F)
DNT-mediated specific killing (%)
IgG1
anti-ICAM-1
Ctrl + DNT
shSOCS1 + DNT
% Increase in DNT killing due to shSOCS1
G)
% Increase in DNT killing after IFNγ treatment
Control
ICAM-1 KO
H)
IgG1
anti-ICAM-1
% Increase in DNT killing after IFNγ treatment
% Increase in Tconv cell killing after IFNγ treatment
OCI-AML2
OCI-AML3
MV4-11
I)
100857
130714
130794
090271
140118
% Increase in DNT killing after IFNγ treatment
IgG1
anti-ICAM-1
ns
J)
r2 = 0.4510
p < 0.0001
% Increase in DNT killing after IFNγ treatment
OCI-AML2
130794
MV4-11
OCI-AML3
090271
090271
100857
150099
KG-1a
140118
090620
130714
ICAM-1 MFI (fold change)

Figure 5

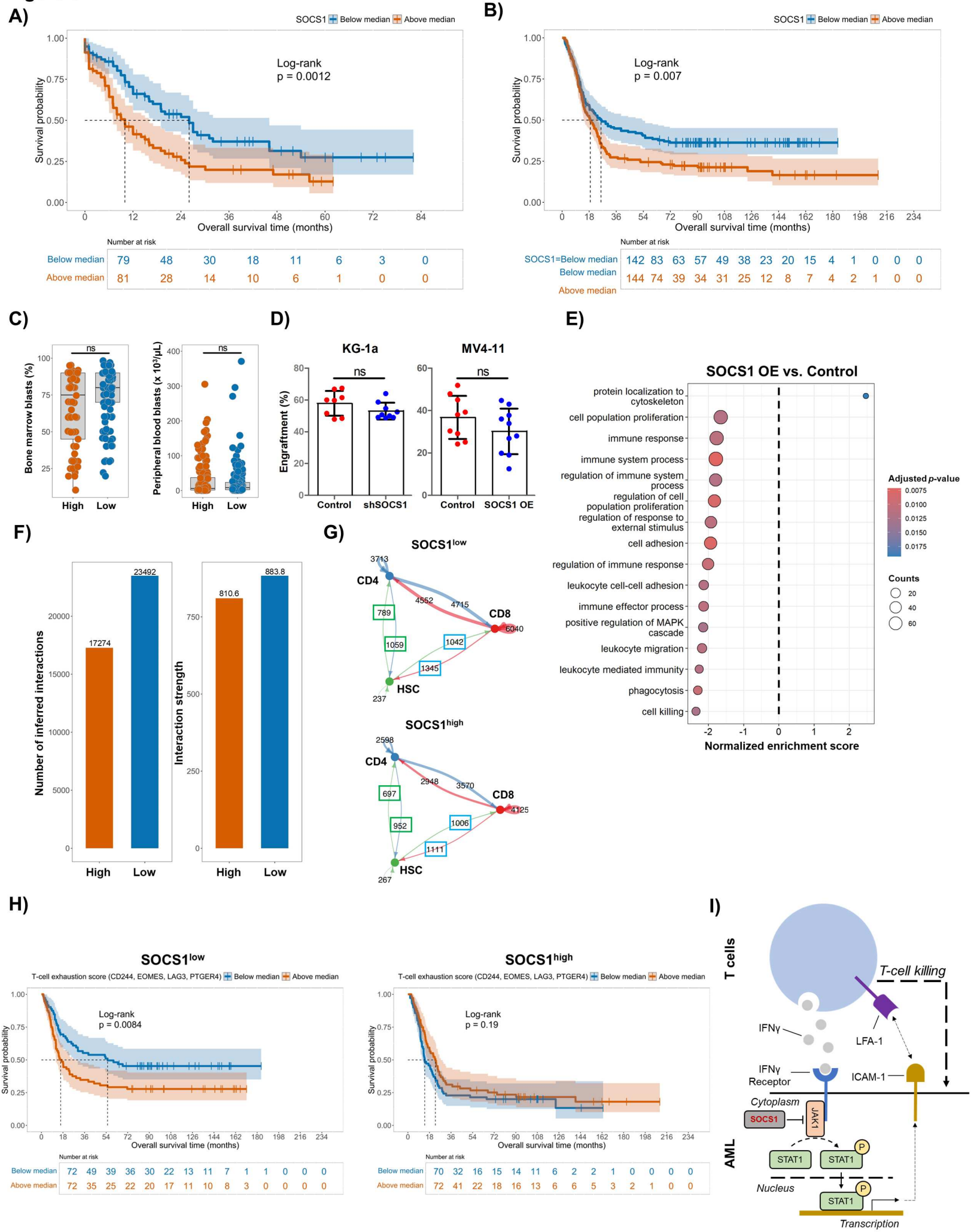
A)
SOCS1 Below median Above median
Log-rank
p = 0.0012
Survival probability
Overall survival time (months)
Number at risk
Below median 79 48 30 18 11 6 3 0
Above median 81 28 14 10 6 1 0 0
B)
SOCS1 Below median Above median
Log-rank
p = 0.007
Survival probability
Overall survival time (months)
Number at risk
SOCS1=Below median 142 83 63 57 49 38 23 20 15 4 1 0 0 0
Below median 144 74 39 34 31 25 12 8 7 4 2 1 0 0
Above median
C)
Bone marrow blasts (%)
Peripheral blood blasts (x 10³/μL)
ns
High Low
D)
KG-1a
MV4-11
Engraftment (%)
ns
Control shSOCS1
Control SOCS1 OE
E)
SOCS1 OE vs. Control
protein localization to cytoskeleton
cell population proliferation
immune response
immune system process
regulation of immune system process
regulation of cell population proliferation
regulation of response to external stimulus
cell adhesion
regulation of immune response
leukocyte cell-cell adhesion
immune effector process
positive regulation of MAPK cascade
leukocyte migration
leukocyte mediated immunity
phagocytosis
cell killing
Normalized enrichment score
Adjusted p-value
0.0075
0.0100
0.0125
0.0150
0.0175
Counts
20
40
60
F)
Number of inferred interactions
17274
23492
Interaction strength
810.6
883.8
High Low
G)
SOCS1low
3713
CD4
4552
4715
CD8
6040
789
1059
1042
1345
HSC
237
SOCS1high
2598
CD4
2948
3570
CD8
4125
697
952
1006
1111
HSC
267
H)
SOCS1low
T-cell exhaustion score (CD244, EOMES, LAG3, PTGER4) Below median Above median
Log-rank
p = 0.0084
Survival probability
Overall survival time (months)
Number at risk
Below median 72 49 39 36 30 22 13 11 7 1 1 0 0 0
Above median 72 35 25 22 20 17 11 10 8 3 0 0 0 0
SOCS1high
T-cell exhaustion score (CD244, EOMES, LAG3, PTGER4) Below median Above median
Log-rank
p = 0.19
Survival probability
Overall survival time (months)
Number at risk
Below median 70 32 16 15 14 11 6 2 2 1 0 0 0 0
Above median 72 41 22 18 16 13 6 6 5 3 2 1 0 0
I)
T cells
T-cell killing
IFNγ
LFA-1
IFNγ Receptor
ICAM-1
Cytoplasm
SOCS1
JAK1
AML
STAT1
STAT1
P
Nucleus
STAT1
P
Transcription